IMPACT EP 24949

D2: Specification of the Inverse Method

DATE	September 3, 1999
ABSTRACT	The document gives a detailed specification of the inverse method including both theory and numerical implementation.
AUTHOR, COMPANY	The IMPACT Consortium under the KTH responsibility
FILING CODE	IMPACT/ART-018-DOC-R1.2
KEYWORDS	Inverse scattering, adjoint state, optimal control
RELATED ITEMS	None
DOCUMENT HISTORY	

Release	Date	Reason of change	Status	Distribution
1.0	2 June 1998	First version	Draft	Internal
1.1	16 June 1998	Introduction and optimisation sections modified	Near final	Internal
1.2	31 July 1998	Summary added, small modifications	Final	Project

Summary

We address the problem of time-domain inverse scattering, where we want to determine some unknown characteristics of an object from measurements of the reflected field. The IMPACT inverse method is described first in a general case in section 1 and then applied to three different solvers for vibro-acoustics, pure acoustics and electromagnetics in sections 2-4. In section 5 the optimisation problem and the structure of the code is discussed. Relating to the workplan, section 1 corresponds to task 1.5, sections 2-4 to the tasks 1.2 and 1.3 and section 5 to task 1.4. The description of the direct codes are kept in appendices A-C. The contents of section 1-5 are summarised in the following.

1. General approach. The inverse scattering problem is stated as an optimal control problem where we want to find the parameter p_{opt} (some characteristics of the scattering object) which minimises the energy norm of the residual between the known and the computed response. Thus p_{opt} is found in an optimisation procedure where in each main iteration the direct problem is solved to obtain the computed response and the parameters are updated in order to minimise the objective function.

Since the direct problem is usually costly to compute it is crucial to limit the number of iterations in the optimisation procedure. In the IMPACT method the gradient of the cost function with respect to the parameters is accurately computed each iteration allowing the use of effective optimisation algorithms such as conjugate gradient and quasi-Newton. The gradient formulas are derived from the Lagrangian of the problem and are found to be:

$$\frac{\partial j}{\partial p_i} = <\mathbf{\Lambda}, \frac{\partial \mathbf{M}(p_i)}{\partial p_i}\mathbf{U}>$$

where p_i are the parameters, $j(p_i)$ the cost function, $\mathbf{\Lambda}$ the Lagrange multipliers or adjoint state, $\mathbf{U}$ the direct state and $\mathbf{M}(p_i)$ the direct state operator. The direct state $\mathbf{U}$ is obtained by solving the direct scattering problem and the dual state by solving the adjoint problem:

$$\mathbf{M}^*(\mathbf{p})\mathbf{\Lambda} = (\mathbf{U} - \mathbf{U}^{obs})$$

where $\mathbf{U}^{obs}$ is the known (observed) response and $\mathbf{M}^*$ the adjoint operator satisfying:

$$<\mathbf{MU}, \mathbf{\Lambda}> = <\mathbf{U}, \mathbf{M}^*\mathbf{\Lambda}>$$

The adjoint problem is typically very similar to direct problem but is solved backwards in time with the residual between known and computed fields as excitation. The same numerical scheme is used as for the direct problem.

2. Aerospatiale: Coupled vibro-acoustic scattering. The problem studied by Aerospatiale is a coupled acoustic and structural problem where the vibrations in a metallic structure subject to an acoustic field are to be minimised. The problem may be described by the system:

$$\begin{cases} \Delta w_{diff} + \frac{1}{c^2}\frac{\partial^2 w_{diff}}{\partial t^2} = 0 & \text{in the whole space} \\ \frac{\partial w_{diff}}{\partial n} = -\frac{\partial w_{inc}}{\partial n} + \rho\frac{\partial^2 u}{\partial t^2} & \text{on } \Gamma \end{cases}$$

where w_{diff} is the unknown of the system (scattered pressure), w_{inc} is the given data of the problem (an incident sound wave for example) and u the displacement of the structure. The direct solver is a time-domain boundary element method for the acoustic problem coupled with a code for the structural problem. The parameter to be optimised is the thickness of the metallic structure. The discrete gradient expression for the thickness parameter as well as the discrete adjoint coupled problem are derived.

3. CRS4: Acoustic scattering. CRS4 studies acoustic wave propagation in inhomogeneous media for determination of the velocity field of the media. The problem is described by the scalar wave equation:

$$\left[\frac{1}{c^2(x,y,z)}\partial_{tt} - \nabla^2\right] P(x,y,z,t) = s(x,y,z,t), \quad t \in (0,T)\,,(x,y,z) \in \Omega$$

where $P(x,y,z,t)$ is the pressure, $c(x,y,z)$ the sound velocity and $s(x,y,z,t)$ the incident wave-field. The numerical scheme used for the direct scattering problem is a high order compact finite-difference scheme. The discrete algorithm for the adjoint problem is derived as well as the gradient expression for the velocity. The problem of exceedingly large number of parameters due to determination of a three dimensional velocity field is addressed and the implications of parametrising the velocity field are considered.

4. KTH: Electromagnetic scattering. KTH studies 2-D electromagnetic wave scattering for reconstruction of dielectric characteristics as well as optimisation of geometrical parameters. The problem is described by Maxwell's equations in 2-D. For the TM-mode they are:

$$\begin{cases} \mu\frac{\partial H_x}{\partial t} &= -\frac{\partial E_z}{\partial y} \\ \mu\frac{\partial H_y}{\partial t} &= \frac{\partial E_z}{\partial x} \\ \varepsilon\frac{\partial E_z}{\partial t} &= \frac{\partial H_y}{\partial x} - \frac{\partial H_x}{\partial y} - \sigma E_z \end{cases}$$

where H_x and H_y are the magnetic fields, E_z the electric field, ε the permittivity, μ the permeability and σ the conductivity. The FD-TD (finite difference in time-domain) method, which is explicit finite difference scheme on a uniform Cartesian mesh, is employed for the numerical solution of the direct problem. The parameters of interest are the dielectric properties of the media but may also be, for example, the thickness of layers in the geometry under study. The case of dispersive media where the dielectric parameters are frequency dependent is also considered and leads to additional parameters.

The discrete adjoint equations are derived and are found to differ from the direct equations only by sign. The same numerical scheme with minor modifications may thus be used for solving the adjoint problem. The discrete gradients for the material parameters are also derived.

5. Optimisation In this section the common (to all applications) optimisation problem is considered. Issues such as regularisation and the computationally costly line-search sub-problem are addressed and different gradient-based algorithms are described in appendix D. The conclusion is that practical experiences are necessary before a definite choice of optimiser (or optimisers) can be made.

Contents

1 Introduction

In the inverse scattering problem we wish to determine some unknown characteristics of the geometry under study from the knowledge of the reflected field. Applications of this problem include non-destructive characterisation of media (for example finding the distribution of oil or gas in the ground or determining the dielectric parameters of an unknown material) and optimisation of material properties or shapes (for example the design of radar absorbing materials or optimising geometrical parameters to avoid vibrations or noise in acoustics).

A possible way of solving the inverse scattering problem is to solve the direct scattering problem in an iterative minimisation procedure where the objective function to be minimised is defined by some norm of the error between simulated and known response. The control variables are the parameters $\mathbf{p}$ describing the unknown characteristics.

This report will describe the general IMPACT approach, which is independent of the choice of direct solver, as well as derive the specific algorithms for three different applications. A brief description of the different sections:

- **1 Introduction.** Includes a description of the general IMPACT approach.
- **2-4 Applications.** Describes the IMPACT algorithm applied to three different applications, the vibro-acoustic coupled problem (Aerospatiale), acoustics (CRS4) and electromagnetics (KTH). These sections include the definition of the direct problem, parameters, cost function, adjoint problem and gradients for each application.
- **5 Optimisers.** Gradient based optimisation, line search, bounds on the parameters.

The specific IMPACT implementation of the inverse algorithm is based on the accurate computation of the gradient of the objective function each minimisation iteration. Information about the gradient is necessary to be able to use effective optimisers such as quasi-Newton and conjugate gradient in the minimisation procedure. We will now describe the IMPACT approach. Observe that the description is kept independent of the choice of direct solver.

The following notation will be used:

$$\begin{aligned}
\mathbf{p} &: \text{ the material parameters} \\
\mathbf{U} &: \text{ the direct state variables} \\
\mathbf{M}(\mathbf{p}) &: \text{ the direct time-domain operator} \\
\mathbf{S_{inc}} &: \text{ the excitation for the direct scattering problem}
\end{aligned}$$

Further, we define the objective function to be minimised as the energy norm in time and space of the error between computed and known response:

$$j(\mathbf{U}(\mathbf{p})) = \frac{1}{2}\int_\Omega \int_T (\mathbf{U} - \mathbf{U}^{obs})^2 \delta(\mathbf{r} - \mathbf{r}_{obs})\, dt\, d\Omega$$

The inverse problem may then be stated as:

Find $\mathbf{p}_{opt}$ for which:

$$j(\mathbf{U}(\mathbf{p}_{opt})) = \min j(\mathbf{U}(\mathbf{p}))$$

under the direct equations constraint:

$$\mathbf{M}(\mathbf{p})\mathbf{U} = \mathbf{S}_{inc} \tag{1}$$

This constrained optimisation problem may be reformulated as the equivalent problem of searching the saddle point of the associated Lagrangian:

$$\mathcal{L}(\mathbf{p}, \mathbf{U}, \mathbf{\Lambda}) = j(\mathbf{U}) + \int_\Omega \int_T \mathbf{\Lambda}(\mathbf{M}(\mathbf{p})\mathbf{U} - \mathbf{S}_{inc})\, dt\, d\Omega \tag{2}$$

where $\mathbf{\Lambda}$ are the Lagrange multipliers or adjoint variables. The direct and adjoint state equations may now be stated as stationary point conditions of the Lagrangian:

$$\nabla_{\mathbf{\Lambda}} \mathcal{L}(\mathbf{p}, \mathbf{U}, \mathbf{\Lambda}) = \mathbf{0} \tag{3}$$

yields the direct equations:

$$\mathbf{M}(\mathbf{p})\mathbf{U} - \mathbf{S}_{inc} = 0$$

and similarly the condition

$$\nabla_{\mathbf{U}} \mathcal{L}(\mathbf{p}, \mathbf{U}, \mathbf{\Lambda}) = \mathbf{0} \tag{4}$$

results in the adjoint equations:

$$\mathbf{M}^*(\mathbf{p})\mathbf{\Lambda} = (\mathbf{U} - \mathbf{U}^{obs})(\mathbf{r}_{obs}, t) \tag{5}$$

where $\mathbf{M}^*$ is the adjoint state operator. Next we derive the gradients of $j(\mathbf{p})$ on the saddle point of the Lagrangian. Let $\mathbf{U} = \mathbf{U}(\mathbf{p})$ be a solution to the direct state equations. The Lagrangian then reduces to:

$$\mathcal{L}(\mathbf{p}, \mathbf{U}(\mathbf{p}), \mathbf{\Lambda}(\mathbf{p})) = j(\mathbf{p})$$

Using the chain rule and the conditions (3) and (4) we obtain:

$$\frac{\partial j}{\partial p_i} = \frac{d\mathcal{L}}{dp_i} = \frac{\partial \mathbf{U}^T}{\partial p_i} \nabla_{\mathbf{U}} \mathcal{L} + \frac{\partial \mathbf{\Lambda}^T}{\partial p_i} \nabla_{\mathbf{\Lambda}} \mathcal{L} + \frac{\partial \mathcal{L}}{\partial p_i} = \frac{\partial \mathcal{L}}{\partial p_i}$$

From the definition of the Lagrangian (2) the gradients then become:

$$\frac{\partial j}{\partial p_i} = \int_\Omega \int_T \mathbf{\Lambda} \frac{\partial \mathbf{M}(p_i)}{\partial p_i} \mathbf{U}\, dt\, d\Omega \tag{6}$$

The adjoint state variables $\mathbf{\Lambda}$ are not available from the solution of the direct problem (1). It is therefore necessary to solve the adjoint problem (5) in order to compute the gradients in (6). The adjoint problem is very similar to the direct problem and is solved using the same numerical algorithm (for example if FDTD is used for the direct problem FDTD is also used for the adjoint equations). The main difference is that the adjoint problem is solved backwards in time using the error as excitation.

The resulting algorithm is illustrated by a block diagram:

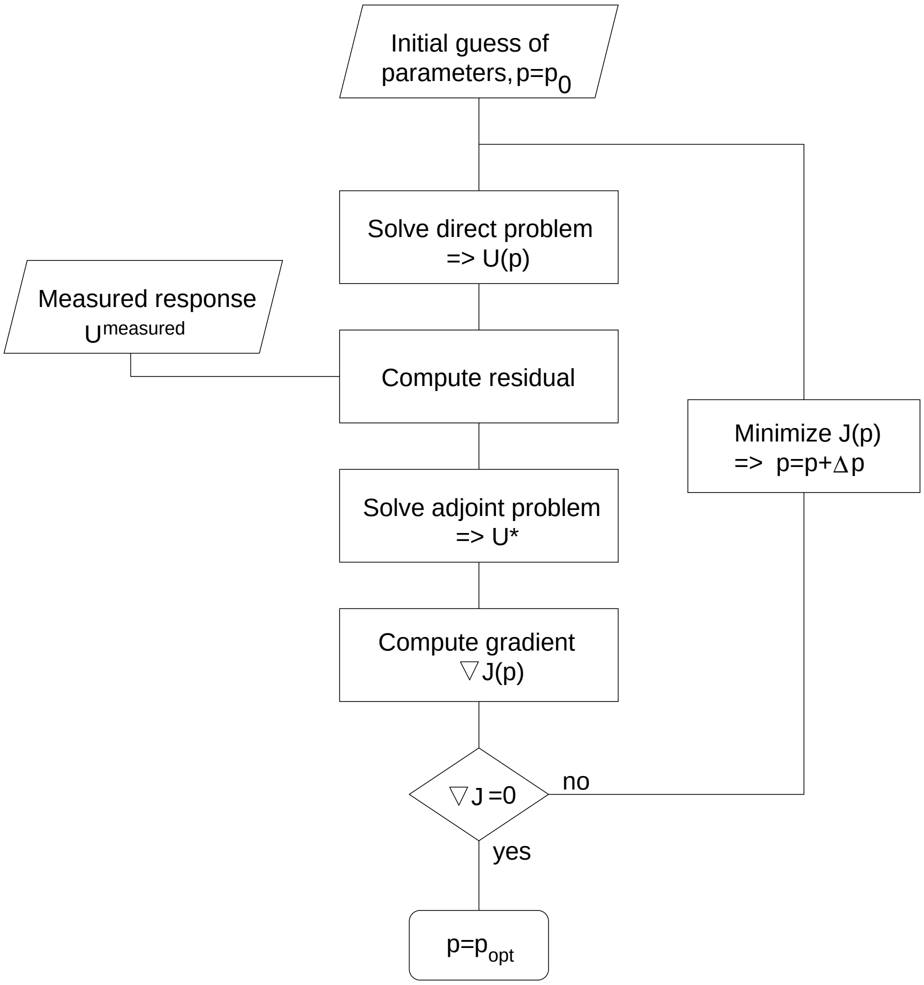

Figure 1: *The IMPACT algorithm for the inverse scattering problem.*

In the discrete case the gradient integrals (6) become sums over all time-levels and all the spatial points where $\mathbf{p}$ is defined. This implies that we must store the direct and adjoint fields in all these points in time and space. It is thus reasonable to ask if a simply computing the gradients as:

$$\frac{\partial j}{\partial p_i} = \frac{j(\mathbf{p} + \Delta p_i \mathbf{e}_i) - j(\mathbf{p})}{\Delta p_i} \tag{7}$$

is not more effective. However, this approach uses one additional direct computation for each parameter. If the number of parameters is more than just a few this method will thus be very ineffective. The poor accuracy of the approximation (7) may also lead to slower convergence in the minimisation procedure. Conclusively (6) is to be preferred in most cases but both ways of computing the gradient will be considered in the validation of the inverse algorithm.

2 Vibroacoustic inverse scattering (Aerospatiale)

2.1 The Direct problem

2.1.1 The vibroacoustic coupled problem

Given an object S with boundary Γ embedded in a flood (air most of the time). The vibroacoustic flood-structure interaction is solved by the following system:

$$\begin{cases} \Delta w_{diff} + \frac{1}{c^2}\frac{\partial^2 w_{diff}}{\partial t^2} = 0 & \text{in the whole space} \\ \frac{\partial w_{diff}}{\partial n} = -\frac{\partial w_{inc}}{\partial n} + \rho \frac{\partial^2 u}{\partial t^2} & \text{on } \Gamma \end{cases}$$

where w_{diff} is the unknown of the system (scattered pressure), w_{inc} is a data of the problem (an incident sounding wave for example), and u the displacement of the structure.
The condition on Γ means that the total normal velocity $v = \frac{\partial w_{tot}}{\partial n}$ is equal to the second time derivative of the displacement u, is the kinematic slip condition of the inviscid fluid on the structure S, as a flexible membrane.
The speed of sound wave propagation in the medium is denoted by c ($c = 340m.s^{-1}$ in the air). ρ is the medium acoustic density.
For the structure, the classical virtual work principle leads to the following classical formulation in terms of the displacement field on the surface :

$$Z_p u + D([w]) = F$$

where Z_p is the mechanical impedance of the structure S, which is related to the stiffness A, the mass E and damping B operators of the structure by the relation :

$$Z_p = A + B\frac{\partial}{\partial t} + E\frac{\partial^2}{\partial t^2}$$

F is the external potential energy, D the potential coupling energy between the structure and the surrounding acoustic medium, $[w]$ the pressure jump.

2.1.2 The acoustic problem

2.1.2.1 Weak Formulation In this formulation, $g = -\frac{\partial w_{inc}}{\partial n} + \rho\frac{\partial^2 u}{\partial t^2}$ is the data of the problem and $g \in H^3(R^+, H^{-1/2}(\Gamma))$ and we search a function $\Phi \in H^2(R^+, H^{1/2}(\Gamma))$ such that for all Ψ in the same space (Φ is the weak solution corresponding to the jump of the w pressure classical solution, across Γ) , we have :

$$\begin{aligned} &\int_R \int_{\Gamma\times\Gamma} \frac{\vec{n}(X).\vec{n}(Y)}{4\pi|X-Y|}\frac{\partial^2\Phi}{\partial t^2}(Y, t - \frac{|X-Y|}{c})\frac{\partial\Psi}{\partial t}(X,t)\ dXdYdt \\ &+c^2\int_R\int_{\Gamma\times\Gamma}\frac{1}{4\pi|X-Y|}\vec{rot}_\Gamma\Phi(Y,t-\frac{|X-Y|}{c})\vec{rot}_\Gamma\frac{\partial\Psi}{\partial t}(X,t)\ dXdYdt \\ &= \int_R\int_\Gamma g(X,t)\frac{\partial\Psi}{\partial t}(X,t)\ dXdt \end{aligned}$$

2.1.2.2 Discretization in time Basis functions are denoted $\gamma^n(t)$ $(n \geq 1)$ and are defined on the figure 2.
We also define the function $\chi_n(t)$ $(n \geq 0)$ whose graph is plotted on the figure 3.
Then, we have :

$$\begin{aligned} \frac{\partial\gamma_n}{\partial t} &= [\chi_{n-1} - \chi_n] \\ \frac{\partial^2\gamma_n}{\partial t^2} &= [\delta_{t_{n+1}} - 2\delta_{t_n} + \delta_{t_{n-1}}] \end{aligned}$$

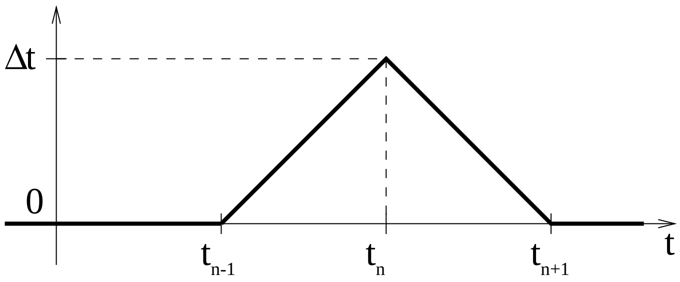

Figure 2: Profile of the function γ_n

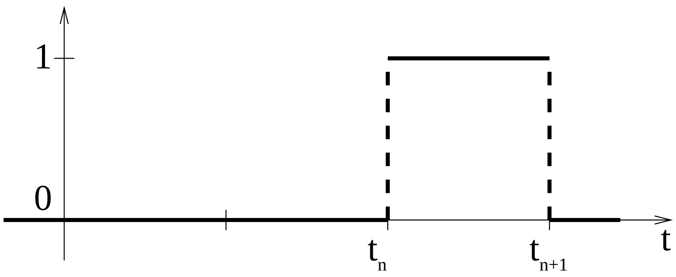

Figure 3: Profile of the function χ_n

2.1.2.3 Discretization in space The equation is solved in space by a surface finite element method. The boundary Γ of the object is meshed with N_h triangular elements. A P1 discretization in space is used. Each basis function φ_i is associated with one vertex S_i, and is defined by :

$$\begin{cases} \varphi_i(S_j) = 1 \text{ if } i = j \text{ and } 0 \text{ otherwise} \\ \varphi_i \text{ is P1 on each triangle} \end{cases}$$

$\varphi_j(M)$ is the barycentric coordinate of M on the vertex j. Let $\overrightarrow{n_j}$ and $\overrightarrow{t_j}$ respectively be the normal and tangent for the edge $[S_j S_{j+1}]$, then we have the expression for φ_j :

$$\varphi_j(M) = \frac{\overrightarrow{S_{j-1}M}.\overrightarrow{n_{j+1}}}{\overrightarrow{S_{j-1}S_j}.\overrightarrow{n_{j+1}}}$$

2.1.2.4 Notation Let :

$$\Phi(X,t) = \sum_{1 \le j \le N_h} \sum_{m \ge 1} a_j^m \gamma_m(t) \varphi_j(X)$$

and let Ψ , the test function defined by :

$$\frac{\partial \Psi}{\partial t}(X,t) = \chi_{n-1}(t) \varphi_i(X)$$

2.1.2.5 Linear system Let X^m be the solution vector at the date t^m : $X^m = [w_j^m]_{1 \le j \le N_h}$. For each time step t^n $(n \ge 1)$ the following linear system is solved :

$$\sum_{m=\sup(1,n-2-L/\Delta t)}^{n} M^{n-m}.X^m = G^n$$

and the right hand side is:

$$G_i^n = \int_{t_{n-1} \le t \le t_n} \int_\Gamma g(X,t).\varphi_i(X) \; dX dt$$

with the matrix M^k :

$$\begin{aligned} M_{ij}^k &= \int_{\Gamma\times\Gamma} \frac{\vec{n}(X).\vec{n}(Y)}{4\pi|X-Y|}\varphi_i(X)\varphi_j(Y) \\ & \left[\chi^0(\frac{|X-Y|}{c}-t_k) - 2\chi^0(\frac{|X-Y|}{c}-t_{k-1}) + \chi^0(\frac{|X-Y|}{c}-t_{k-2})\right] dXdYdt \\ & + c^2\int_0^{\Delta t}\int_{\Gamma\times\Gamma}\frac{\vec{rot}\varphi_i(X)\vec{rot}\varphi_j(Y)}{4\pi|X-Y|}\gamma_1(t+t_k-\frac{|X-Y|}{c})\ dXdYdt \end{aligned}$$

For example, with n=3, the system becomes :

$$M^2.X^1 + M^1.X^2 + M^0.X^3 = G^3$$

where the only unknown is X^3.
We clearly see three contributions in the system :

- The term G^n is representative of the excitation (or other data) ;
- The term $\sum_{1\leq m\leq n-1} M^{n-m}.X^m$ is representative of the past contribution ;
- The term $M^0.X^n$ is the present contribution, to compute

Physically, the expression of this equation is explained by the fact that what occurs at the date n (*i.e.* X^n) is a consequence of what occurred at the date $(n-m)$ on the elements situated at a distance $m.c.\Delta t$ (*i.e.* X^{n-m}) for all $n > 1$. Mathematically, this causality link is contained in the expression of the matrices M^k. Indeed, M^k is representative of the interactions between elements situated at a distance $k.c.\Delta t$ each other. Therefore :

- (M^k) are sparse (for a given element e_1, the elements e_2 situated at a distance $k.c.\Delta t$ from e_1 do not constitute an important portion of the mesh) ;
- M^0 is almost diagonal (because it only takes account the self-interaction of elements or eventually with their nearby neighbours;
- The (M^k) have an aspect plotted on the figure 4.

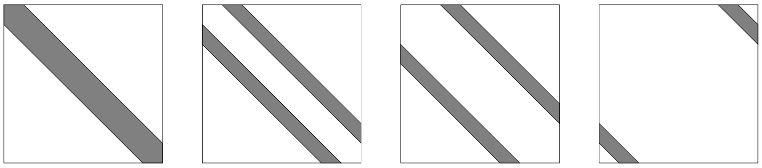

Figure 4: Aspect of the matrices M^k

2.1.2.6 Matrices M^k

The matrices M^k can be developed in the following expressions:

$$\begin{aligned} M_{ij}^k &= \int\int_{t_k\leq\frac{|X-Y|}{c}\leq t_{k+1}} \frac{\vec{n}(X).\vec{n}(Y)}{4\pi|X-Y|}\varphi_i(X)\varphi_j(Y)dXdY \\ & -2\int\int_{t_{k-1}\leq\frac{|X-Y|}{c}\leq t_k} \frac{\vec{n}(X).\vec{n}(Y)}{4\pi|X-Y|}\varphi_i(X)\varphi_j(Y)dXdY \\ & +\int\int_{t_{k-2}\leq\frac{|X-Y|}{c}\leq t_{k-1}} \frac{\vec{n}(X).\vec{n}(Y)}{4\pi|X-Y|}\varphi_i(X)\varphi_j(Y)dXdY \\ & +\int\int_{t_k\leq\frac{|X-Y|}{c}\leq t_{k+1}} \frac{\vec{rot}\varphi_i(X)\vec{rot}\varphi_j(Y)}{4\pi|X-Y|}\frac{1}{2}(c.t_k-|X-Y|+c.\Delta t)^2 \end{aligned}$$

$$+\int\int_{t_{k-1}\leq\frac{|X-Y|}{c}\leq t_k}\frac{\vec{rot}\varphi_i(X)\vec{rot}\varphi_j(Y)}{4\pi|X-Y|}\frac{1}{2}(c^2.\Delta t^2-2(c.t_k-|X-Y|)^2+2c.\Delta t(c.t_k-|X-Y|))$$
$$+\int\int_{t_{k-2}\leq\frac{|X-Y|}{c}\leq t_{k-1}}\frac{\vec{rot}\varphi_i(X)\vec{rot}\varphi_j(Y)}{4\pi|X-Y|}\frac{1}{2}(c.t_k-|X-Y|-2c.\Delta t)^2$$

2.1.2.7 Near field pressure computation Denote by H the 3D time domain Green function

$$G(x,t)=\frac{1}{4\pi}\frac{\delta\,(t-|x|)}{|x|}$$

Define the integral double layer operator K, for Φ a regular function defined on Γ (solution of the variational equation above and with time domain representation X^m), and for an exterior point x by :

$$K\Phi(x,t)=\int_R\int_\Gamma\frac{\partial G}{\partial n_y}(x-y,t-\tau)\Phi(y,\tau)d\Gamma_y d\tau$$

Then the acoustic near field (pressure) w, solution of the original coupled problem, can be computed by :

$$w=K\Phi(x,t)$$

2.1.2.8 Excitations The code can treat two kind of excitations :

sinusoidal excitation : $s(t)=sin(\omega.t)$

gaussian excitation : $s(t)$ can be written :

$$s(t)=exp(-\pi\left(\frac{ct-\frac{c}{f}\sqrt{-\frac{log\alpha}{\pi}}\sqrt{-\frac{logD}{\pi}}}{\frac{c}{f}\sqrt{-\frac{log\alpha}{\pi}}}\right)^2)$$

f is the maximum propagating frequency. D and $s(0)$ represents the discontinuity at $t=0$. Finally, α is the FFT value of the function $s()$ at the frequency f. Most of the time $\alpha=0,1$ and $D=0,01$.

2.1.3 The structural problem

Recall that for the structure S, the classical virtual work principle leads to the following classical formulation in terms of the displacement field on the surface :

$$Z_p u+D(w)=F$$

where Z_p is the mechanical impedance of the structure S, F is the external potential energy, D the potential coupling energy between the structure and the surrounding acoustic medium, u the displacement, w the local pressure.
The displacement u is discretized in time at the time $n+\frac{3}{2}$ by $U^{n+\frac{3}{2}}$, for example.
Discretizing the first and second derivative in time just above, we obtain the following explicit scheme : $U^{n+\frac{3}{2}}$ the displacement is computed (by a Newmark hyperbolic scheme in time), as we know the displacement for preceding times and the pressure jump X^n at the time n:

$$K_1U^{n+\frac{3}{2}}+K_2U^{n+\frac{1}{2}}+K_3U^{n-\frac{1}{2}}-D(X^n)=F^{n+\frac{1}{2}}$$

where K_1,K_2,K_3 are new operators and $F^{n+\frac{1}{2}}$ the external discrete potential energy.

2.1.4 Implementation of the coupled direct problem

We give here an example of the coupled direct problem implementation.
First, we compute the structural solution $U^{n+\frac{3}{2}}$ at time $n+\frac{3}{2}$ by :

$$K_1 U^{n+\frac{3}{2}} + K_2 U^{n+\frac{1}{2}} + K_3 U^{n-\frac{1}{2}} - D(X^n) = F^{n+\frac{1}{2}}$$

And then, we update the acoustic part, at time $n+1$. The system becomes (with a virtual three functions) :

$$M^2.X^{n-1} + M^1.X^n + M^0.X^{n+1} = G^{n+1}$$

where the only unknown is X^{n+1} and where G^{n+1} is the excitation at the time $n+1$ and equal to :

$$G^{n+1} = v_{inc}^{n+1} + \rho \frac{u^{n+\frac{3}{2}} - 2u^{n+\frac{1}{2}} + u^{n-\frac{1}{2}}}{\Delta t^2}$$

Then, we update the mechanical part $U^{n+\frac{5}{2}}$, and so on ...
Formally, we solve first at time n, the pressure X^n and then the displacement U_n.

$$\begin{cases} \sum_{m=1}^{n} M_{mn} X^m = V_{inc}{}^n + RU''_{n-1} \\ EU''_n + BU'_n + AU_n = F^n + DX^n \end{cases}$$

2.2 The Inverse problem

2.2.1 Observation datas and parameters

We define the parameter p or control variable (which depends on the medium characteristics : here it is the metallic structure's thickness) and note that $p \in C_{adm}$, where C_{adm} is an admissible set of parameters (a priori information).
Defining formally $M(p)$ as the time domain acoustic operator (depending on p) by :

$$\begin{aligned} M(p) = \quad & \int_R \int_{\Gamma\times\Gamma} \frac{\vec{n}(X).\vec{n}(Y)}{4\pi|X-Y|} \frac{\partial^2}{\partial t^2}(Y, t - \frac{|X-Y|}{c})\ dXdYdt \\ & + c^2 \int_R \int_{\Gamma\times\Gamma} \frac{1}{4\pi|X-Y|} \vec{rot}_\Gamma (Y, t - \frac{|X-Y|}{c}) \vec{rot}_\Gamma\ dXdYdt \end{aligned}$$

The purely acoustic excitation is given by :

$$V_{inc} = -\frac{\partial w_{inc}}{\partial n}$$

The vibro-mechanical excitation is given by :

$$R = \rho \frac{\partial^2}{\partial t^2}$$

then the total acoustic excitation G is $G = V_{inc} + Ru$.
Recall that the mechanical operator Z_p (depending on p) is :

$$Z_p = A + B\frac{\partial}{\partial t} + E\frac{\partial^2}{\partial t^2}$$

F is the external potential energy and D the potential coupling energy between the structure and the surrounding acoustic medium.
The direct state equations are then formally written :

$$\begin{cases} M(p)X = V_{inc} + Ru \\ Z_p U - [D]X = F \end{cases}$$

In the optimal control formulation, the state variable T will be denoted, referring to the direct problem notations above, $T = (U, w)$ which is here the displacement and the acoustic pressure jump.
We note U_{obs} the measurement data.
Denote by $H(p)$ the direct state operator by :

$$H(p) = \begin{pmatrix} M(p) & -R \\ -D & Z_p \end{pmatrix}$$

and by S_{inc} the right hand side excitation :

$$S_{inc} = \begin{pmatrix} V_{inc} \\ F \end{pmatrix}$$

2.2.2 Specification of the objective functional

Defining $Res(T)$ the residual datas on the displacement U :

$$Res(T) = (\sum_{k=1}^{k=N} (U - U_{obs})^2 (\delta_{capt(k),t})$$

where N is the number of measurement points and $\delta_{capt(k)}$ is the position of the point number k. The cost function is written

$$\begin{aligned} j(p) &= J(T(p)) \\ &= \frac{1}{2} < Res(T), Res(T) > \end{aligned}$$

2.2.3 The Lagrangian approach

By the optimal control theory, finding p_{opt} as

$$j(p_{opt}) = \min j(p) \qquad \forall p \in C_{adm}$$

under the state equation constraint, is equivalent to search the saddle point an associated Lagrangian defined below.
Let $Q^* = (X^*, U^*)$ be a costate variable (dual variable). Then the Lagrangian, function of three variables (p, T, Q^*) is

$$\begin{aligned} L(p, T, Q^*) &= J(U) + < Q^*, ([H(p)]T - S_{inc}) > \\ &= \frac{1}{2} < Res(U), Res(U) > \\ &\quad + < X^*, (M(p)X - V_{inc} - Ru) > \\ &\quad + < U^*, (Z_p U - [D]X - F) > \end{aligned}$$

Remark that p and U are completely independent here, the constraint being added via the second term of Lagrangian .
Searching the saddle point of the Lagrangian is searching $(p_{opt}, T_{opt}, T^*_{opt})$ which verify

$$\begin{aligned} &L(p_{opt}, T_{opt}, Q^*_{opt}) \leq L(p_{opt}, T_{opt}, Q^*_{opt}) \leq L(p, T, Q^*_{opt}) \\ &\quad \forall p, T, Q^* \in C_{adm} \end{aligned}$$

If $(p_{opt}, T_{opt}, Q^*_{opt})$ is saddle point of the Lagrangian, then p_{opt} is the optimal control searched.

2.2.4 Definition of the adjoint equation

For each state variable T, the corresponding costate variable T^* verify the first Euler equation

$$\frac{\partial L(p,T,T^*)}{\partial T} = 0$$

then the adjoint (or dual) equations are performed by

$$\left\{ H^*(p)T^* = Res(T) \right.$$

Expliciting the term $H^*(p)$, with the adjoint operators $M^*(p)$,R^*, $(D)^*$, and Z_p^*, we have :

$$H^*(p) = \begin{pmatrix} M^*(p) & -([D])^* \\ -R^* & Z_p^* \end{pmatrix}$$

where

$$\begin{aligned} M^*(p) &= M(p) \\ R^* &= R \\ Z_p^* &= A - B\frac{\partial}{\partial t} + E\frac{\partial^2}{\partial t^2} \end{aligned}$$

and D^* the adjoint operator of D (coupling operator which maps the pressure jump and with a coupling with structural test function).
For the complete final adjoint coupled system, we obtain :

$$\left\{ \begin{array}{l} M^*(p)X^* - (D)^* U^* = 0 \\ Z_p^* U^* - R^* X^* = U - U_{obs} \end{array} \right.$$

2.2.5 Numerical implementation of the adjoint coupled problem

We give here an example of the coupled adjoint problem implementation.
The problem is solved by a time reversal process.
First, we update the acoustic part, at time $n+1$. The system becomes (with a virtual three functions) :

$$M^2.X^*_{n+3} + M^1.X^*_{n+2} + M^0.X^*_{n+1} - D^*(U^n)) = 0$$

where the only unknown is X^*_{n+1}.
Then, we compute the structural solution $U^*_{n+\frac{1}{2}}$ at time $n + \frac{1}{2}$ by :

$$K_1 U^*_{n+\frac{1}{2}} + K_2 U^*_{n+\frac{3}{2}} + K_3 U^*_{n+\frac{5}{2}} = \rho \frac{X^*_{n+1} - 2X^*_{n+2} + X^*_{n+3}}{\Delta t^2}$$

And then, we update the acoustic part, at time n, and so on ...
Formally, we solve first at time n, the displacement U_n^* and then the pressure X_n^*.

$$\left\{ \begin{array}{l} \sum_{m=n}^{n+k} M_{mn} X_m^* = DU_n^* \\ EU^{*''}_n - BU^{*'}_n + AU_n^* = Res(U_n) + RX^{*''}_{n+1} \end{array} \right.$$

2.2.6 Computation of the gradients

If T and p are in relation with the state equation, denote by $T = T(p)$ the solution to

$$\left\{ H(p)T = S_{inc} \right.$$

The Lagrangian is then simplified in

$$L(p,T,T^*) = j(p)$$

Computing the gradients of j, for the parameter p, we have

$$\nabla j(p)\delta p = \left(\frac{\partial L}{\partial p}\delta p + \frac{\partial L}{\partial T}T^{'}\delta p\right)(p, T, T^*)$$

Now, with the relation

$$\frac{\partial L(p, T, T^*)}{\partial T} = 0$$

gradient formulas are obtained :

$$\begin{aligned}
\frac{\nabla j}{\nabla p} &= \frac{\partial}{\partial p}L(p, T, T^*) \\
&= < Q^*, \left(\frac{\partial [H(p)]}{\partial p}T\right) > \\
&= + < X^*, \left(\frac{\partial M(p)}{\partial p}X\right) > \\
&\quad + < U^*, \left(\frac{\partial Z_p}{\partial p}U\right) >
\end{aligned}$$

2.2.7 Application for the thickness structural parameter

The only term depending of the thickness p is the mass matrix of the structural operator Z_p. In fact we have :

$$\begin{aligned}
\frac{\nabla j}{\nabla p} &= \frac{\partial}{\partial p}L(p, T, T^*) \\
&= < Q^*, \left(\frac{\partial [H(p)]}{\partial p}T\right) > \\
&= < U^*, \left(\frac{\partial A(p)}{\partial p}U\right) >
\end{aligned}$$

For the discrete gradient, we obtain :

$$\begin{aligned}
\frac{\nabla j}{\nabla p} &= \\
&= \sum_{n=1}^{ntmax} < U_n^*, \left(\frac{\partial A(p)}{\partial p}U_n\right) >
\end{aligned}$$

3 Acoustic inverse scattering (CRS4)

3.1 The direct code and the energy–tuned absorbing boundaries

3.1.1 Introduction

In acoustic modelling, the study of wave phenomena in a bounded domain $\Omega \subset \mathcal{R}^3$, with sound velocity c and constant density, is based on the solution of the scalar wave equation

$$\left(\partial_{tt} - c^2(x,y,z)\nabla^2\right) P(x,y,z,t) = 0 \quad t \in (0,T)\,, \quad (x,y,z) \in \Omega \tag{8}$$

with initial conditions $P\,(x,y,z,0) = P_0\,(x,y,z)$ and $\partial_t P\,(x,y,z,0) = Q_0\,(x,y,z)$. Setting $Q = \partial_t P$, the second order equation can be reformulated as a first order system corresponding to the Hamilton equations for wave propagation:

$$\begin{aligned} \partial_t P &= Q, \\ \partial_t Q &= c^2\nabla^2 P. \end{aligned} \tag{9}$$

From this we can derive the continuity equation

$$\frac{dH}{dt} = \int_{\partial\Omega} Q\,\vec{\nabla}P \cdot d\vec{\sigma} \tag{10}$$

where $H(t) = \frac{1}{2}\int_\Omega \left((\vec{\nabla P})^2 + (Q/c)^2\right) dV$ is interpreted as the energy inside Ω at time t and $\vec{J} = -Q\vec{\nabla}P$ as the local energy flux density. If $\vec{J}\cdot d\vec{\sigma}$ vanishes everywhere on the boundary $\partial\Omega$, then $dH/dt = 0$ and energy is conserved. Otherwise, wherever $\vec{J}$ points outward, energy decreases locally and wherever $\vec{J}$ points inward, energy increases locally [?]. From these observations follows a necessary energy condition for absorption at a boundary: $dH/dt \leq 0$.

A well-established way of imposing this condition and implementing an absorbing boundary is based on the observation that an impulse traveling along direction $\hat{n}$ with velocity c satisfies the simplest paraxial wave equation (Sommerfeld's radiation condition [?])

$$\partial_t P + c\hat{n}\cdot\vec{\nabla}P = 0. \tag{11}$$

Imposing Eqn(**??**) on $\partial\Omega$ and identifying $\hat{n}$ as the normal to the boundary, we see that $dH/dt \leq 0$ is indeed satisfied. This does not, however, prevent the existence of reflected waves corresponding to other (non-normal) wave angles. This can be quantified by the reflection coefficient for a plane monochromatic wave impinging a flat boundary, $R = -(1-\cos\theta)/(1+\cos\theta)$, where $\theta \in [0, \pi/2]$ is the angle between the normal to the boundary and the wave vector.

Our strategy for constraining *all* waves to be absorbed by the boundary is to solve the wave equation (**??**) also on $\partial\Omega$ and then impose $\vec{J}\cdot\hat{n} \geq 0$ by locally reversing the sign of Q on the boundary wherever the projection of $\vec{J}$ along the normal $\hat{n}$ is negative:

$$\mathrm{FOR}\ \ (\mathrm{x,y,z}) \in \partial\Omega\ \ \mathrm{WHERE}\ \ \vec{\mathrm{J}}\cdot\hat{\mathrm{n}} < 0\ \ \mathrm{DO}\ \ \mathrm{Q(x,y,z,t)} \leftarrow -\ \mathrm{Q(x,y,z,t)}. \tag{12}$$

The use of this mechanism ensures that the energy contained inside Ω does not increase in time. By way of illustration, we consider a bounded domain Σ which contains Ω and with a reflecting boundary $\partial\Sigma$, Figure (**??**). An impulsive wave from inside Ω approaches the boundary $\partial\Omega$ and $\vec{J}\cdot\hat{n} \leq 0$ will be true there; mechanism (**??**) changes nothing and $\partial\Omega$ is a perfectly transparent boundary. Once the wave hits $\partial\Sigma$, its reflected component bounces back to $\partial\Omega$ with $\vec{J}\cdot\hat{n} > 0$; then the reversal of Q transforms $\partial\Omega$ into a reflecting boundary.

Remark that while the energy evolution is altered by reversing the sign of Q, the instantaneous value of the energy is not, and conservation of energy is intact. In contrast to Eqn(**??**), this mechanism also preserves the local energy flux strength $\parallel \vec{J} \parallel$.

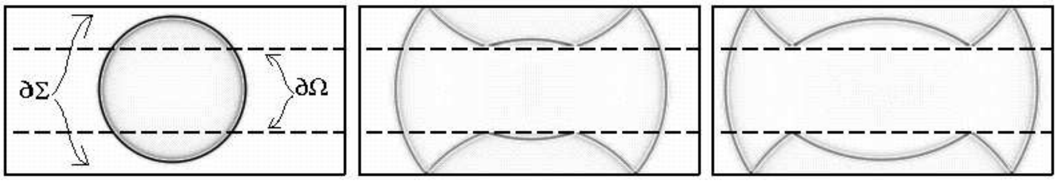

Figure 5: Boundary transparent in the outward direction and reflecting in the inward direction.

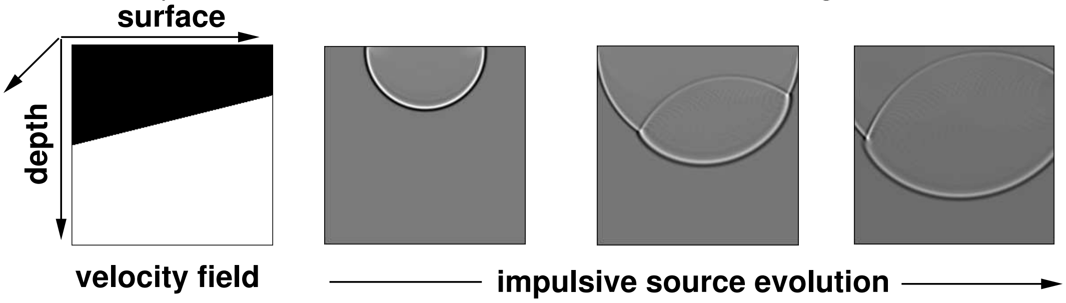

Figure 6: Energy-tuned absorbing boundary condition: $256 \times 256 \times 256$ mesh points.

3.1.2 Numerical implementation

Mechanism (**??**), the main ingredient of the absorbing boundary that we propose, can be easily applied using the Hamiltonian formulation of wave propagation because the generalized momentum Q is treated as an independent field. We consider a class of reversible discrete approximations to Hamilton's equations (**??**) and give both stability and dispersion conditions [**?**]. For instance, the following fourth order accurate time integration scheme

$$\left\{ \begin{array}{lclcl} Q^{(n+\frac{1}{3})} & = & Q^{(n)} & + & \frac{1}{6}\,\Delta t c^2 \nabla^2 P^{(n)} \\ P^{(n+\frac{1}{2})} & = & P^{(n)} & + & \frac{1}{2}\,\Delta t Q^{(n+\frac{1}{3})} \\ Q^{(n+\frac{2}{3})} & = & Q^{(n+\frac{1}{3})} & + & \frac{2}{3}\,\Delta t c^2 \nabla^2 P^{(n+\frac{1}{2})} \\ P^{(n+1)} & = & P^{(n+\frac{1}{2})} & + & \frac{1}{2}\,\Delta t Q^{(n+\frac{2}{3})} \\ Q^{(n+1)} & = & Q^{(n+\frac{2}{3})} & + & \frac{1}{6}\,\Delta t c^2 \nabla^2 P^{(n+1)}, \end{array} \right. \tag{13}$$

leads to the 3D stability condition $c\Delta t/min(\Delta x, \Delta y, \Delta z) \leq \theta$, where θ depends on the spatial discretization scheme. Values of θ corresponding to spectral schemes, sixth order compact differences [**?**] and fourth and second order central differences are reported in the table. Moreover, imposing a 1% tolerance between the physical and numerical dispersion relations, we find a region of allowable stepsizes that respect this tolerance [**?**]. This leads us to the coarsest possible discretization for a stable method which respects the desired tolerance: $\Delta t_{max} = 1/(p_t f)$ and $max(\Delta x, \Delta y, \Delta z) = c/(pf)$, where f is the maximum frequency present in the spectrum of the initial data. The values of p and p_t, also reported in the table, are identified respectively as the number of wavelengths per gridpoint and samples per period necessary for avoiding numerical dispersion.

Mechanism (**??**) is now rendered effective by extending the Q reversal to all points of $\Sigma \backslash \Omega$. Numerical experiments confirm that energy is then trapped in a strip pattern inside this layer. To dissipate this unwanted energy, which is a source of numerical error, we implement the simplest absorbing boundary, Eqn(**??**), discretized with finite differences, on $\partial\Sigma$. Figure (**??**) shows a simulation which uses this mechanism. We have used an absorbing layer on the order of ten meshpoints in each direction. Computer experiments indicate that optimal thickness depends only weakly on the size of the computational grid. To summarize, a single time integration step consists of the following three phases: integrating the Hamiltonian equations in Σ, imposing mechanism (**??**) in $\Sigma \backslash \Omega$ and damping the residual energy by integrating the paraxial equation (**??**) on $\partial\Sigma$. Because the algorithm constrains energy not to increase in time, the solution is guaranteed to be bounded by the initial data, thus ensuring well-posedness of the approach [**?**].

	spectral	**compact**	**IV FD**	**II FD**
θ	0.45	0.54	0.61	0.71
p_t	7.85	4.56	5.15	15.54
p	$*$	2.5	3.17	11.02

3.2 The inverse problem

3.2.1 The continuum formulation

Reconstructive imaging can be considered to involve two components: the forward problem and the inverse problem. In the forward problem defined by the propagation model, acoustic or electromagnetic, an estimate of the model parameters is used to numerically propagate signals, producing synthetic data. The comparison between synthetic and experimental data gives a measure of the quality of the model. However, it is not always clear how to use this information to update and correct model parameters. The inverse problem is thus designed to furnish an algorithm for automatically inferring model parameters from real and synthetic data, resulting in more reliable imaging.
In non-elastic acoustic modeling, the study of wave phenomena in a bounded domain $\Omega \subset \mathcal{R}^3$, with sound velocity c and constant density, is based on the solution of the scalar wave equation

$$\left[\frac{1}{c^2(x,y,z)}\partial_{tt} - \nabla^2\right] P(x,y,z,t) = s(x,y,z,t), \quad t \in (0,T)\,,(x,y,z) \in \Omega \tag{14}$$

with initial conditions $P(x,y,z,0) = \partial_t P(x,y,z,0) = 0$. Wavefield s represents the impulsive source described as follows:

$$s\,(x,y,z,t) = \delta(t) q\,(x,y,z) + \delta'(t) p\,(x,y,z)\,. \tag{15}$$

Acoustic inversion attempts to find the velocity field c that minimizes the difference between synthetic and experimental data. A measure of this discrepancy, evaluated on the horizontal acquisition plane $z = z_0$, is obtained by the norm

$$E\,[P,c] = \frac{1}{2}\int_\Omega dx\; dy\; dz \int_0^T dt\left[P(x,y,z,t) - \tilde{P}(x,y,z,t)\right]^2 \delta(z - z_0). \tag{16}$$

In this expression, $\tilde{P}$ represents the experimental data and P the synthetic wave traveling at velocity c, obtained by integrating equation (**??**).
Because the minimization of the error function (**??**) is constrained by the evolution law of P, we use the Lagrange multiplier technique to search for the optimal field c. For this purpose, we introduce a new objective functional, the Lagrangian

$$J\,[\lambda,P,c] = E\,[P,c] + \int_\Omega dx\; dy\; dz \int_0^T dt\;\lambda\;\left[\left(-\frac{1}{c^2}\partial_{tt} + \nabla^2\right) P + s\right]. \tag{17}$$

The solution of the inverse problem is found at the stationary point of J with respect to $\lambda(x,y,z,t)$, $P(x,y,z,t)$ and $c(x,y,z,t)$. ¿From the computation of the variation of J with respect to λ, namely $\delta J/\delta\lambda = 0$, we recover the forward problem defined by equations (**??**) and (**??**).
To calculate the variation of J with respect to P, we first observe that under the following conditions [1]

$$\int_{\partial\Omega}\left(\lambda\vec{\nabla}P + P\vec{\nabla}\lambda\right)\cdot d\vec{\sigma} = 0, \qquad \lambda\,(T) = \partial_t\lambda\,(T) = 0, \tag{18}$$

it is possible to derive the identity

$$\int_\Omega dx\; dy\; dz \int_0^T dt\;\left[\lambda\;\left(-\frac{1}{c^2}\partial_{tt} + \nabla^2\right) P - P\left(-\frac{1}{c^2}\partial_{tt} + \nabla^2\right)\lambda\right] = 0. \tag{19}$$

Introducing equation (**??**) in (**??**), from the computation of $\delta J/\delta P = 0$ we obtain the adjoint problem defined as follows:

$$\left[\frac{1}{c^2(x,y,z)}\partial_{tt} - \nabla^2\right]\lambda(x,y,z,t) = S(x,y,z,t), \quad t \in (0,T)\,,(x,y,z) \in \Omega, \tag{20}$$

with final conditions $\lambda(x,y,z,0) = \partial_t\lambda(x,y,z,0) = 0$. The source term represents the difference between synthetic and experimental data, evaluated on the acquisition plane at $z = z_0$:

$$S(x,y,z,t) = \left[P(x,y,z,t) - \tilde{P}(x,y,z,t)\right]\delta(z - z_0). \tag{21}$$

[1] This is the self-adjointness condition for the differential operator $\left(-\frac{1}{c^2}\partial_{tt} + \nabla^2\right)$

Depending on which boundary conditions are imposed to the forward problem, boundary conditions for the adjoint problem must be constrained by the surface condition in (**??**).
Finally, the variation of J with respect to c gives the gradient

$$\frac{\delta J}{\delta c}(x,y,z) = -\frac{2}{c^3}\int_0^T dt\ \partial_t\lambda\ \partial_t P. \tag{22}$$

A heuristic solution of the inverse problem, leading to the search for the velocity field c minimizing (**??**), is obtained by the following iterative procedure:

1. the computation of P, solution of (**??**);
2. the computation of λ, solution (**??**);
3. the computation of the gradient (**??**);
4. the update of the velocity field using a descent method:

$$c^{(n+1)} = c^{(n)} - \alpha^{(n)}\frac{\delta J}{\delta c}^{(n)}. \tag{23}$$

Starting from an initial guess $c^{(0)}$ hopefully not very far from the optimum c, we construct a sequence $c^{(n)}$, equation (**??**), that should converge to the closest fixed point to $c^{(0)}$. At the present moment, no theory provides information about the nature of the solution, existence and uniqueness, and the convergence of the above iterative process.

3.2.2 The discrete formulation

The adopted discrete time evolution scheme (see description in appendix **??**), introducing the Hamiltonian conjugate field Q, it is represented by the following equation (we omitted for clarity the space dependencies):

$$\left\{\begin{array}{lcllc} Q^{(n+\frac{1}{3})} & = & Q^{(n)} & + & \frac{1}{6}\,\Delta t c^2\left(\nabla^2 P^{(n)} + s^n\right) \\ P^{(n+\frac{1}{2})} & = & P^{(n)} & + & \frac{1}{2}\,\Delta t Q^{(n+\frac{1}{3})} \\ Q^{(n+\frac{2}{3})} & = & Q^{(n+\frac{1}{3})} & + & \frac{2}{3}\,\Delta t c^2\left(\nabla^2 P^{(n+\frac{1}{2})} + s^n\right) \\ P^{(n+1)} & = & P^{(n+\frac{1}{2})} & + & \frac{1}{2}\,\Delta t Q^{(n+\frac{2}{3})} \\ Q^{(n+1)} & = & Q^{(n+\frac{2}{3})} & + & \frac{1}{6}\,\Delta t c^2\left(\nabla^2 P^{(n+1)} + s^n\right) \end{array}\right. \tag{24}$$

with zero initial condition,

$$P^0 = Q^0 = 0, \tag{25}$$

The source term, s^n, is defined, as in the continuum case, by:

$$s^n(x,y,z) = p(x,y,z)f'(n\Delta t) + q(x,y,z)f(n\Delta t), \tag{26}$$

where the function $f(t)$ represents a band limited approximation of the Dirac delta $\delta(t)$, typically a gaussian.
This mapping may be written in the matrix form, useful for further mathematical elaboration:

$$\left\{\begin{array}{l} \vec{u}^{\,n+1} = \mathbf{A}\,(c\,)\,\vec{u}^{\,n} + \vec{b}^{\,n}, \\ \vec{u}^{\,0} = 0, \end{array}\right. \tag{27}$$

where $\vec{u}^{\,n}$ represents the vector with components

$$\vec{u}^{\,n} = \begin{pmatrix} P^n \\ Q^n \end{pmatrix}, \tag{28}$$

and $\vec{b}^{\,n}$ is a source term connected to s^n. The operator $\mathbf{A}$ is defined as:

$$\mathbf{A} = \begin{pmatrix} 1+\frac{1}{2}\sigma+\frac{1}{36}\sigma^2 & \Delta t\left(1+\frac{1}{6}\sigma\right) \\ \Delta t^{-1}\left(\sigma+\frac{1}{36}\sigma^2+\frac{1}{216}\sigma^3\right) & 1+\frac{1}{2}\sigma+\frac{1}{36}\sigma^2 \end{pmatrix} \tag{29}$$

where the operator σ is given by:

$$\sigma = \Delta t^2 \; c^2 \; \nabla^2. \tag{30}$$

The ∇^2 operator, once selected the appropriate space discretization scheme, will be represented by a matrix $\mathcal{D}$.
Now, the objective functional, which contains the constraint (??) via a Lagrange multiplier $\vec{\Lambda}^{\;n}$,

$$\vec{\Lambda}^{\;n} = \left(\begin{array}{c} \lambda^n \\ \lambda^{*n} \end{array} \right), \tag{31}$$

is written as:

$$J\left[\vec{\Lambda}^{\;n}, \vec{u}^{\;n}, c\right] = \sum_n \left[\frac{1}{2} ||\vec{u}^{\;n} - \vec{u}_0^{\;n}||^2 + \left(\vec{\Lambda}^{\;n}, \vec{u}^{\;n+1} - \mathbf{A}\left(c\right) \vec{u}^{\;n} - \vec{b}^{\;n} \right) \right], \tag{32}$$

where $(\vec{v},\vec{w}) = \int_\Omega \vec{v}(x,y,z) \cdot \vec{w}(x,y,z) \; dx \; dy \; dz$ is the scalar product obtained by integrating over all space points, $||v||^2 = (\vec{v},\vec{v})$ the norm and $\vec{u}_0^{\;n}$ represents the experimental data measured at the surface $z = 0$.
As usual, the differentiation of the Lagrangian with respect to its three independent variables, imposing to zero the resulting derivatives, lead us to the constitutive equations for the inverse problem.
The derivative with respect to the adjoint field $\vec{\Lambda}^{\;n}$ imposed equal to zero will simply give the time evolution scheme, (??). The derivative with respect to the direct field $\vec{u}^{\;n}$ gives the following equation:

$$\vec{\Lambda}^{\;n-1} - \mathbf{A}\left(c\right)^\dagger \vec{\Lambda}^{\;n} = -\left(\vec{u}^{\;n} - \vec{u}_0^{\;n}\right) \tag{33}$$

with zero initial conditions, $\vec{\Lambda}^0 = 0$. Operator $\mathbf{A}\left(c\right)^\dagger$ represents the adjoint of the operator $\mathbf{A}\left(c\right)$, and is given by:

$$\mathbf{A}^\dagger = \left(\begin{array}{cc} 1 + \frac{1}{2}\sigma^\dagger + \frac{1}{36}\sigma^{\dagger 2} & \Delta t^{-1}\left(\sigma^\dagger + \frac{1}{36}\sigma^{\dagger 2} + \frac{1}{216}\sigma^{\dagger 3}\right) \\ \Delta t\left(1 + \frac{1}{6}\sigma^\dagger\right) & 1 + \frac{1}{2}\sigma^\dagger + \frac{1}{36}\sigma^{\dagger 2} \end{array} \right) \tag{34}$$

Equation (??) perfectly agrees with its continuum counterpart, (??): it represents an extrapolation backward in time with a source term given by the difference between the measured and the simulated data. In particular, if the space is infinite or fields are zero at the boundaries, $\sigma = \sigma^\dagger$, thus all the matrix element operators of $\mathbf{A}^\dagger$, are self–adjoint, $\mathbf{A}\left(c\right)^\dagger_{ij} = \mathbf{A}\left(c\right)_{ij}$, that implies that, with slight changes, *the same scheme used for the direct solver have to be used in the adjoint solver*, equation (??). In the space discretized version the Laplacian, ∇^2 operator, will be substituted by its discrete counterpart $\mathcal{D}$, thus the adjoint operator $\mathbf{A}^\dagger$ will be based on the use of the transposed matrix $\mathcal{D}^t$.
Finally, the derivative with respect to the velocity field will give the condition for updating the gradient:

$$\frac{\partial J}{\partial c} = -\sum_n \left(\vec{\Lambda}^{\;n}, \frac{\partial \mathbf{A}\left(c\right)}{\partial c} \vec{u}^{\;n} \right). \tag{35}$$

Equation (??) should be used, instead of its continuum counterpart, (??), to evaluate the gradient coherently with the discrete approach. In any case, for small Δt, the differences between different schemes to evaluate time derivatives inside the integral/sum, should be negligible.

3.2.3 Computation of the gradients

Reconstructive imaging can be considered to involve two components: the forward problem and the inverse problem. In the forward problem defined by the propagation model, acoustic or electromagnetic, an estimate of the model parameters is used to numerically propagate signals, producing synthetic data. The comparison between synthetic and experimental data gives a measure of the quality of the model. However, it is not always clear how to use this information to update and correct model parameters. The inverse problem is thus designed to furnish an algorithm for automatically inferring model parameters from real and synthetic data, resulting in more reliable imaging.
Let us denote by $f(u(p))$ the norm of the error between simulated and acquired data:

$$f(u(p)) = \frac{1}{2}||u(p) - u_{msr}||^2.$$

Field $u(p)$ is solution of the direct equation described by a differential operator D:

$$D(p)u = 0.$$

The parameter field p, the input of the simulation model, is unknown and must be determined by the inverse problem. The comparison between synthetic and experimental data gives a measure of the quality of the inference of p. The aim of the inversion procedure is to minimize this norm, with respect to p, with the constraint imposed by the direct model. We can rephrase the problem as an unconstrained problem by introducing the Lagrangian multiplier λ to construct a new objective function,

$$\mathcal{L}(p, u, \lambda) = \frac{1}{2}||u - u_{msr}||^2 + (\lambda, D(p)u),$$

where p, u and λ are now independent fields. We are now looking for the saddle point of the Lagrangian $\mathcal{L}$, minimizing along p and u directions and maximizing along λ direction. Setting to zero the gradient with respect to λ, we obviously obtain the
direct equation model $D(p)u = 0$. Setting to zero the gradient with respect to u, we obtain the so called adjoint equation:

$$D^\dagger(p)\lambda = -(u - u_{msr}).$$

The gradient with respect to p takes the form:

$$\frac{\partial \mathcal{L}}{\partial p} = \left(\lambda, \frac{\partial D}{\partial p} u\right).$$

Observe that for a fixed field p, assuming $u(p)$ solution of the direct prob lem, the evaluation of the Lagrangian $\mathcal{L}$ gives

$$f(u(p)) = \mathcal{L}\,(p, u(p), \lambda)$$

Moreover, the expression of the gradient of $\mathcal{L}$ with respect to p, evaluated for a fixed p with $u(p)$ and $\lambda(p)$ solutions respectively of the direct and adjoint problems, takes the form

$$\delta\mathcal{L}\,(p, u(p), \lambda(p)) = \frac{\partial \mathcal{L}\,(p, u(p), \lambda(p))}{\partial p}\delta p = \frac{\partial f\,(u(p))}{\partial p}\delta p.$$

¿From this last relation, we deduce the important result:

$$\frac{\partial f\,(u(p))}{\partial p} = \frac{\partial \mathcal{L}\,(p, u(p), \lambda(p))}{\partial p}.$$

Notice that the adjoint solution $\lambda(p)$ is exclusively necessary for the expensive computation of the gradient of $f\,(u(p))$ required by the large family of minimization algorithms presented, for instance in document T1.4.

In non-elastic acoustic modelling, the study of wave phenomena in a bounded domain, with sound velocity $c(x, y, z)$ and constant density, is based on the solution of the scalar wave equation.

Acoustic inversion attempts to find the velocity field c that minimizes the difference between synthetic and experimental data. In this context c plays the role of field parameter p. In conformity with the inverse problem Lagrangian formulation, we have that the variation of $\mathcal{L}$ with respect to c gives the following gradient expression

$$\frac{\partial \mathcal{L}}{\partial c}(x, y, z) = -\frac{2}{c^3}\int_0^T dt\ \partial_t\lambda(x, y, z, t)\ \partial_t P(x, y, z, t).$$

Recalling that the solution of the adjoint problem $\lambda(x, y, z, t)$ is performed in reverse time, the computation of the time integral, for each point (x, y, z), requires the storing of the entire history of both direct and adjoint solutions. So, without any simplification, the numerical computation of the gradient, particularly in 3D, can be an intractable problem.

For this reason, we see three main strategies, to surmount this difficulty.

3.2.3.1 Evaluation of the gradient in the Fourier domain This idea is based on the observation that the gradient is a convolution of two fields, then resulting in a multiplication in the Fourier space. In fact, if we define the function $\lambda(x,y,z,t) = \tilde{\lambda}(x,y,z,T-t)$, we may express

$$\frac{\partial \mathcal{L}}{\partial c}(x,y,z) = \frac{2}{c^3}(\partial_t \tilde{\lambda}) \otimes_t (\partial_t P)(x,y,z,T) = \frac{2}{c^3}\int d\omega \left[\widehat{\partial_t \tilde{\lambda}}\ \widehat{\partial_t P}\right] e^{i\omega T}$$

In this way we need to store *all* the data, as before, but "compressed" by Fourier transform in time. The drawback is that now we need to perform all the necessary DFTs forward and backward in time. DFT should be partially evaluated and stored at each time step.

3.2.3.2 Evaluation of the gradient by intermediate field storage: lossy and loss-less cases In the very simple case of a lossless equation, we may evaluate the gradient integral with no disk storage, dynamically in memory. Infact, in this case, we solve the field equation and keep only the field P at the final time T. Thus, back-propagating P from T, with 'final' condition $P(x,y,z,T)$, to 0 and, simultaneously, the field λ, we have both fields P and λ accessible at the same evaluation time! The main drawback is that we need to solve one more direct equation in reverse time.
To avoid round–off errors or to take into account small information losses, we can divide the interval $[0,T]$ in a definite number of sub–intervals, $[t_i, t_{i+1}]$ and store the direct evolution of P at each steps t_i. In this case, the approach is to solve backward in time, inside the interval $[t_i, t_{i+1}]$, both the P field (starting from the final condition $P(x,y,z,t_{i+1})$) and the λ field. The two fields are then known at the same evaluation times and then it's possible compute the contribution to gradient in this time interval. In the case of lossy equations, the obtained result will be an approximation.
If the propagation is lossy, as it is the case of the acoustic wave equation with absorbing boundaries, the correct procedure directly comes from the preceding considerations. As before, we perform a direct run and store the field P only at the intermediate steps, $P(x,y,z,t_i)$. Then, we solve the direct field P *forward* in time in the time interval $[t_i, t_{i+1}]$ jointly with the conjugated field λ *backward* in time in the same interval. In this way we evaluate the partial gradient by reversing, for instance λ, inside $[t_i, t_{i+1}]$. This strategy leads to a reduced disk storage or, if the RAM is sufficient, to an in–core execution.

3.2.3.3 Parametrization of the velocity field To simplify the updating procedure, we may reduce the number of parameters by defining the velocity field in terms of some function set. For instance we may use a parametric interpolation of the velocity defined on a collection of N points $q_1, q_2, \ldots, q_N$ inside the spatial domain under consideration:

$$c(x,y,z) = \sum_{i=1}^{N} c_i \phi_i(x,y,z), \text{ where } \phi_i(q_j) = \delta_{ij},$$

ϕ_i are shape functions and $c_1, c_2, \ldots, c_N$, the new parameters to be determined, may be interpreted as the values of the velocity field on the collection of points $q_1, q_2, \ldots, q_N$.
Now, the straightforward derivative of the Lagrangian (implicit function derivation rule) gives:

$$\frac{\partial \mathcal{L}}{\partial c_i} = \int_\Omega dx\ dy\ dz\ \frac{\partial \mathcal{L}}{\partial c(x,y,z)} \frac{\partial c(x,y,z)}{\partial c_i}$$

In the example of the interpolation it gives:

$$\frac{\partial \mathcal{L}}{\partial c_i} = -\int_\Omega dx\ dy\ dz\ \frac{2}{c^3}\phi_i(x,y,z) \int_0^T dt\ \partial_t \lambda(x,y,z,t)\ \partial_t P(x,y,z,t).$$

If the function ϕ_i have a support $D_i = \{(x,y,z) | \phi_i(x,y,z) \neq 0\}$, then:

$$\frac{\partial \mathcal{L}}{\partial c_i} = -\int_{D_i} dx\ dy\ dz\ \frac{2}{c^3}\phi_i(x,y,z) \int_0^T dt\ \partial_t \lambda(x,y,z,t)\ \partial_t P(x,y,z,t).$$

Thus, to evaluate the gradient we need to know the field P and λ not in all the bulk Ω, but in each support D_i. If $vol(D_i) << vol(\Omega)$, this results in a reduced storage requirements

$$(\mathrm{vol}(\cup_{i=0}^{N} D_i) \times N_t)\ :\ (\mathrm{vol}(\Omega) \times N_t)$$

The space integral is then evaluated on a coarser grid (with respect to that used for discretizing the propagation equations) by a numerical quadrature.

4 Electromagnetic inverse scattering (KTH)

4.1 Introduction

The problem we wish to study is the inverse scattering of electromagnetic waves in time-domain. By solving this problem it is possible to determine unknown object parameters from measurements of the field reflected by the object. Examples of applications include non-destructive reconstruction of dielectric properties and optimisation of shape or material to minimise reflection.

Section **??** describes the direct scattering problem, both the continuous governing equations and the numerical scheme, FDTD, that is employed for their solution. A more detailed description of FDTD is included in appendix **??**. In section **??** the inverse method is explained, based on the Lagrangian approach described in the introduction of the main document.

4.2 The direct problem

4.2.1 The Maxwell equations

The time-dependent electromagnetic field is governed by the Maxwell equations:

$$\begin{aligned} -\frac{\partial \mathbf{B}}{\partial t} &= \nabla \times \mathbf{E} && (36) \\ \frac{\partial \mathbf{D}}{\partial t} &= \nabla \times \mathbf{H} - \mathbf{J} && (37) \\ \nabla \cdot \mathbf{D} &= \rho \\ \nabla \cdot \mathbf{B} &= 0 \end{aligned}$$

where $\mathbf{E}$ is the electric field in V/m, $\mathbf{D}$ the electric flux density in C/m^2, $\mathbf{H}$ the magnetic field in A/m, $\mathbf{B}$ the magnetic flux density in Vs/m^2, $\mathbf{J}$ the electric current density in A/m^2 and ρ the charge density in C/m^3.

In linear, isotropic and non-dispersive media the constitutive relations between the fields and the fluxes are:

$$\begin{aligned} \mathbf{B} &= \mu \mathbf{H} \\ \mathbf{D} &= \varepsilon \mathbf{E} \\ \mathbf{J} &= \sigma \mathbf{E} \end{aligned} \qquad (38)$$

where the permittivity ε, the permeability μ and the conductivity σ are constant in time but may vary in space. Substituting these relations into equations (**??**) and (**??**) results in:

$$\begin{aligned} -\mu \frac{\partial \mathbf{H}}{\partial t} &= \nabla \times \mathbf{E} && (39) \\ \varepsilon \frac{\partial \mathbf{E}}{\partial t} &= \nabla \times \mathbf{H} - \sigma \mathbf{E} && (40) \end{aligned}$$

In two dimensions (**??**) and (**??**) decouple into two separate systems, the transverse magnetic, TM mode and the transverse electric, TE mode. We state here only the TM mode:

$$\begin{aligned} \mu \frac{\partial H_x}{\partial t} &= -\frac{\partial E_z}{\partial y} && (41) \\ \mu \frac{\partial H_y}{\partial t} &= \frac{\partial E_z}{\partial x} && (42) \\ \varepsilon \frac{\partial E_z}{\partial t} &= \frac{\partial H_y}{\partial x} - \frac{\partial H_x}{\partial y} - \sigma E_z && (43) \end{aligned}$$

4.2.2 Dispersive media

In many common media the constitutive parameters ε,μ and σ depend on the frequency of the interacting field. This means that the constitutive relations (**??**) are only valid in the frequency domain since the product between parameter and field becomes a convolution in the time-domain. However, given the frequency dependence model we may Fourier transform the frequency-domain relation into the time-domain. Using that $j\omega$ becomes $\frac{\partial}{\partial t}$ we then obtain an ordinary differential equation. For Debye dispersive media the permittivity is given by:

$$\varepsilon(\omega) = \varepsilon_\infty + \frac{\varepsilon_s - \varepsilon_\infty}{1 + j\omega t_0}$$

The relation between **D** and **E** may then be written on the form of an ordinary differential equation in the time-domain. The system of equations to solve in the TM case then becomes:

$$\begin{aligned}
\mu\tfrac{\partial H_x}{\partial t} + \tfrac{\partial E_z}{\partial y} &= 0\\
\mu\tfrac{\partial H_y}{\partial t} - \tfrac{\partial E_z}{\partial x} &= 0\\
\tfrac{\partial D_z}{\partial t} - \tfrac{\partial H_y}{\partial x} + \tfrac{\partial H_x}{\partial y} + \sigma E_z &= 0\\
a\tfrac{\partial D_z}{\partial t} + b\tfrac{\partial E_z}{\partial t} + D_z + cE_z &= 0
\end{aligned}$$

where t_0, ε_s and ε_∞ are contained in the coefficients a, b and c. The same approach may be used to treat dispersive permeability and conductivity. Notice that the order of the dispersive model determines the order of the time-derivatives in the auxiliary differential equation.

4.2.3 Numerical method, finite difference in time-domain (FDTD)

The FDTD algorithm solves the Maxwell curl equations (**??**) and (**??**) using an explicit finite difference scheme. It is not necessary to solve the divergence equations since they are implicitly satisfied by the curl equations in the FDTD discretization.

4.2.3.1 Discretisation

In FDTD the spatial derivatives are numerically realised by central finite differences on a uniform Cartesian grid. The discrete electric and magnetic field components are located at separate points in space in order to minimise the number of unknowns without loosing accuracy. The 2D mesh for the TM mode is illustrated in figure **??**.

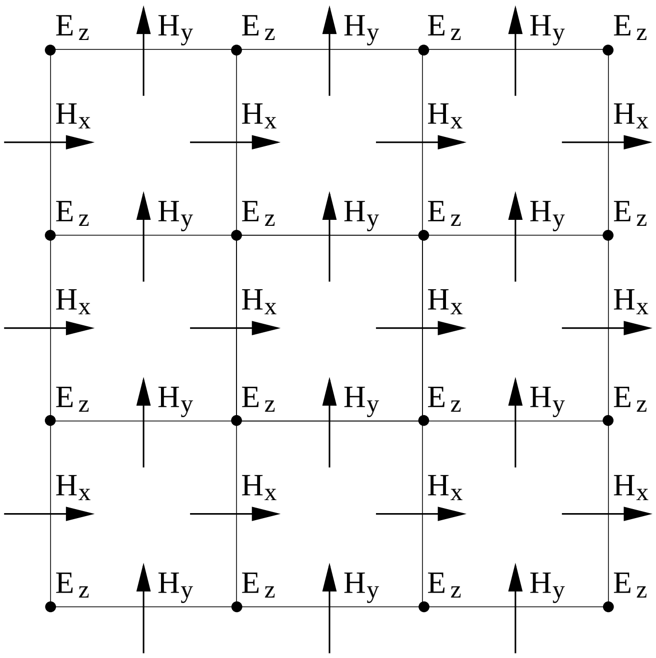

Figure 7: *Staggered grid in 2D (TM).*

Central difference are used in time as well, resulting in a leap-frog numerical scheme, second order accurate in both time and space. The **E** and **H** components are staggered one half time-step. Both the **E** and **H** fields are initially set to zero.
To illustrate the approach we state the time-stepping expressions for the TM mode (**??**)-(**??**):

$$H_x|_{i,j+\frac{1}{2}}^{n+\frac{1}{2}} = H_x|_{i,j+\frac{1}{2}}^{n-\frac{1}{2}} - \frac{\Delta t}{\mu_{i,j+\frac{1}{2}}}\left[\frac{E_z|_{i,j+1}^{n} - E_z|_{i,j}^{n}}{\Delta y}\right]$$

$$H_y|_{i+\frac{1}{2},j}^{n+\frac{1}{2}} = H_y|_{i+\frac{1}{2},j}^{n-\frac{1}{2}} + \frac{\Delta t}{\mu_{i,j+\frac{1}{2}}}\left[\frac{E_z|_{i+1,j}^{n} - E_z|_{i,j}^{n}}{\Delta x}\right]$$

$$E_z|_{i,j}^{n+1} = \left(\frac{1-\frac{\sigma_{i,j}\Delta t}{2\varepsilon_{i,j}}}{1+\frac{\sigma_{i,j}\Delta t}{2\varepsilon_{i,j}}}\right) E_z|_{i,j}^{n} + \\ + \left(\frac{\frac{\Delta t}{\varepsilon_{i,j}}}{1+\frac{\sigma_{i,j}\Delta t}{2\varepsilon_{i,j}}}\right)\left[\begin{array}{c} \frac{H_y|_{i+\frac{1}{2},j}^{n+\frac{1}{2}} - H_y|_{i-\frac{1}{2},j}^{n+\frac{1}{2}}}{\Delta x} \\ -\frac{H_x|_{i,j+\frac{1}{2}}^{n+\frac{1}{2}} - H_x|_{i,j-\frac{1}{2}}^{n+\frac{1}{2}}}{\Delta y}\end{array}\right] \tag{44}$$

In (**??**) the approximation:

$$E_z|_{i,j}^{n+\frac{1}{2}} \approx \frac{E_z|_{i,j}^{n+1} + E_z|_{i,j}^{n}}{2}$$

is used for the E_z field on the right-hand side of equation (**??**).

4.2.3.2 Excitation

Two different types of excitations are used depending on application, point source and plane wave. In both cases the wave form is a Gaussian pulse in time, in order to get a wide frequency range of the response. The point source is modeled by simply adding an excitation term in the update of the electric field component at the location of the source. Plane waves are modeled by Huygens surfaces which are based on a division of the fields in incident and scattered fields, see figure **??**.

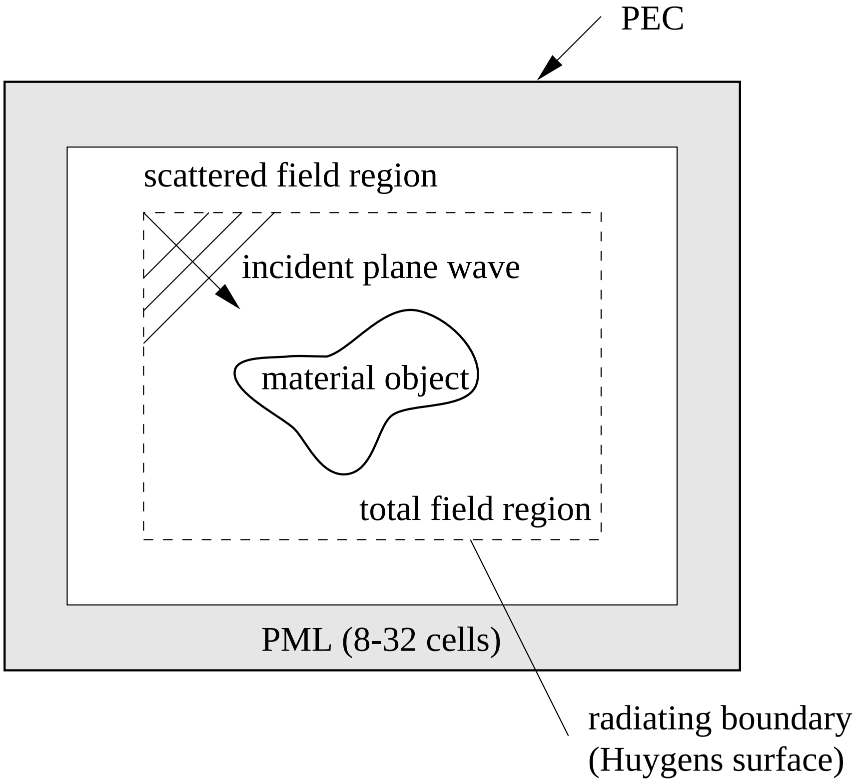

Figure 8: *Computational domain in 2D FDTD.*

4.2.3.3 Boundary conditions

In order to model open domains the uniaxial perfectly matched absorbing layer (U-PML) is used on the boundaries. The U-PML is based on the fact that for a plane wave incident on a uniaxial media it is possible to derive conditions for the permittivity and permeability such that the wave will be purely transmitted into the media. The technique is to enclose the computational domain with a highly lossy layer of such media terminated by an outer PEC (perfect electric conductor) wall, as illustrated in figure **??**.

Metallic boundaries or Perfect Electric Conductors (PEC) are modeled by simply setting the electric field components tangential to the PEC boundary to zero. This implies that the PEC boundaries are always placed in electric field points in the grid.

4.2.3.4 Dispersive media

In dispersive media the auxiliary differential equation (ADE) approach is employed which means solving an extra ordinary differential equation resulting from the time-domain constitutive relations. In Debye media the FDTD equations become:

$$
\begin{aligned}
H_x^{n+\frac{1}{2}}|_{i,j+\frac{1}{2}} &= H_x^{n-\frac{1}{2}}|_{i,j+\frac{1}{2}} - \frac{\Delta t}{\mu|_{i,j+\frac{1}{2}}\Delta y}(E_z^n|i,j+1 - E_z^n|i,j) \\
H_y^{n+\frac{1}{2}}|_{i+\frac{1}{2},j} &= H_y^{n-\frac{1}{2}}|_{i+\frac{1}{2},j} + \frac{\Delta t}{\mu|_{i+\frac{1}{2},j}\Delta x}(E_z^n|i+1,j - E_z^n|i,j) \\
D_z^{n+1}|_{i,j} &= D_z^n|_{i,j} + \frac{\Delta t}{\Delta x}(H_y^{n+\frac{1}{2}}|_{i+\frac{1}{2},j} - H_y^{n+\frac{1}{2}}|_{i-\frac{1}{2},j}) \\
&\quad - \frac{\Delta t}{\Delta y}(H_x^{n+\frac{1}{2}}|_{i,j+\frac{1}{2}} - H_x^{n+\frac{1}{2}}|_{i,j-\frac{1}{2}}) - \frac{\Delta t\sigma|_{i,j}}{2}(E_z^{n+1}|_{i,j} + E_z^n|_{i,j}) \\
E_z^{n+1}|_{i,j} &= \frac{b|_{i,j} - \frac{c|_{i,j}\Delta t}{2}}{b|_{i,j} + \frac{c|_{i,j}\Delta t}{2}} E_z^n|_{i,j} \\
&\quad - \frac{1}{b|_{i,j} + \frac{c|_{i,j}\Delta t}{2}}\left(a|_{i,j}(D_z^{n+1}|_{i,j} - D_z^n|_{i,j}) - \frac{\Delta t}{2}(D_z^{n+1}|_{i,j} + D_z^n|_{i,j})\right)
\end{aligned}
$$

4.3 The inverse problem

4.3.1 Parameters

The inverse algorithm wish to reconstruct the geometrical or material characteristics of the scattering object. We define $\mathbf{p}$ as a vector containing the parameters to be found. In the case of simple non-dispersive media $\mathbf{p}$ may be the permittivity, permeability and conductivity of the object:

$$\mathbf{p} = \begin{pmatrix} \varepsilon \\ \mu \\ \sigma \end{pmatrix}$$

In dispersive Debye media the material parameters are the permeability, the conductivity and the three coefficients in the additional ordinary differential equation:

$$\mathbf{p} = \begin{pmatrix} \mu \\ \sigma \\ a \\ b \\ c \end{pmatrix}$$

4.3.2 Specification of the objective functional

The objective functional in the 2D TM case is defined as:

$$j(\mathbf{p}) = \frac{1}{2}\int_T\int_\Omega \delta_{x^{obs},y^{obs}}(E_z(\mathbf{p}) - E_z^{obs})^2 d\Omega dt$$

where E_z and E_z^{obs} are the computed and measured electric fields at the observation point (x^{obs}, y^{obs}) and $\delta_{x^{obs},y^{obs}} = \delta(x - x^{obs}, y - y^{obs})$ is the Dirac function that picks E_z at the observation point in space.

4.3.3 The Lagrangian approach

The constrained optimisation problem of finding the parameter $\mathbf{p}_{opt}$ satisfying:

$$j(\mathbf{U}(\mathbf{p}_{opt})) = \min j(\mathbf{U}(\mathbf{p}))$$

under the direct state equations constraints is equivalent to searching the saddle point of the associated Lagrangian. In the TM mode for non-dispersive media the Lagrangian is defined as:

$$
\begin{aligned}
L(\mathbf{p},\mathbf{U},\mathbf{U}^*) = \; & \tfrac{1}{2}\int \delta_{x^{obs},y^{obs}}(E_z - E_z^{obs})^2\, d\Omega \\
& + \int H_x^*(\mu \tfrac{\partial H_x}{\partial t} + \tfrac{\partial E_z}{\partial y})\, d\Omega \\
& + \int H_y^*(\mu \tfrac{\partial H_y}{\partial t} - \tfrac{\partial E_z}{\partial x})\, d\Omega \\
& + \int E_z^*(\varepsilon \tfrac{\partial E_z}{\partial t} - \tfrac{\partial H_y}{\partial x} + \tfrac{\partial H_x}{\partial y} + \sigma E_z)\, d\Omega
\end{aligned} \tag{45}
$$

where

$$
\mathbf{U} = \begin{pmatrix} H_x \\ H_y \\ E_z \end{pmatrix} \quad \mathbf{U}^* = \begin{pmatrix} H_x^* \\ H_y^* \\ E_z^* \end{pmatrix} \quad \mathbf{p} = \begin{pmatrix} \varepsilon \\ \mu \\ \sigma \end{pmatrix}
$$

4.3.4 Definition of the adjoint equations

The adjoint equations are given by the stationary point condition of the Lagrangian on the saddle point:

$$
\nabla_{\mathbf{U}}\mathcal{L}(\mathbf{p},\mathbf{U},\mathbf{U}^*) = \mathbf{0}
$$

resulting in the adjoint equations:

$$
\mathbf{M}^*(\mathbf{p})\mathbf{\Lambda} = (\mathbf{U} - \mathbf{U}^{obs})(\mathbf{r}_{obs}, t)
$$

where $\mathbf{M}^*$ is the adjoint differential operator corresponding to the direct state equations (**??**)-(**??**). The adjoint operator satisfies the relation $< MU, U^* > = < U, M^*U^* >$. By partial integration of the constraints terms in (**??**) we thus obtain:

$$
\mathbf{M}^* = \begin{pmatrix} -\mu\frac{\partial}{\partial t} & 0 & -\frac{\partial}{\partial y} \\ 0 & -\mu\frac{\partial}{\partial t} & \frac{\partial}{\partial x} \\ -\frac{\partial}{\partial y} & \frac{\partial}{\partial x} & -\varepsilon\frac{\partial}{\partial t} + \sigma \end{pmatrix}
$$

and the adjoint equations are:

$$
\begin{aligned}
& -\mu\tfrac{\partial H_x^*}{\partial t} - \tfrac{\partial E_z^*}{\partial y} = 0 \\
& -\mu\tfrac{\partial H_y^*}{\partial t} + \tfrac{\partial E_z^*}{\partial x} = 0 \\
& -\varepsilon\tfrac{\partial E_z^*}{\partial t} + \tfrac{\partial H_y^*}{\partial x} - \tfrac{\partial H_x^*}{\partial y} + \sigma\lambda_z = (E_z - E_z^{obs})(x^{obs}, y^{obs}, t)
\end{aligned}
$$

In the same way the adjoint equations in dispersive media may be derived. In the case of Debye media the adjoint equations become:

$$
\begin{aligned}
& -\mu\tfrac{\partial H_x^*}{\partial t} - \tfrac{\partial E_z^*}{\partial y} = 0 \\
& -\mu\tfrac{\partial H_y^*}{\partial t} + \tfrac{\partial E_z^*}{\partial x} = 0 \\
& -b\tfrac{\partial D_z^*}{\partial t} + cD_z^* + \sigma E_z^* - \tfrac{\partial H_x^*}{\partial y} + \tfrac{\partial H_y^*}{\partial x} = (E_z - E_z^{obs})(x^{obs}, y^{obs}, t) \\
& -\tfrac{\partial E_z^*}{\partial t} - a\tfrac{\partial D_z^*}{\partial t} + D_z^* = 0
\end{aligned}
$$

The discrete adjoint equations may be derived in much the same way but instead of integrating by parts we use summation by parts. In the case of non-dispersive media the discrete adjoint equations become:

$$
\begin{aligned}
& -(H_x^{*n+1}|_{i,j+\frac{1}{2}} - H_x^{*n}|_{i,j+\frac{1}{2}}) - \tfrac{\Delta t}{\mu|_{i,j+\frac{1}{2}}\Delta y}(E_z^{*n+\frac{1}{2}}|_{i,j+1} - E_z^{*n+\frac{1}{2}}|_{i,j}) && = 0 \\
& -(H_y^{*n+1}|_{i+\frac{1}{2},j} - H_y^{*n}|_{i+\frac{1}{2},j}) + \tfrac{\Delta t}{\mu|_{i+\frac{1}{2},j}\Delta x}(E_z^{*n+\frac{1}{2}}|_{i+1,j} - E_z^{*n+\frac{1}{2}}|_{i,j}) && = 0 \\
& -\varepsilon|_{i,j}(E_z^{*n+\frac{3}{2}}|_{i,j} - E_z^{*n+\frac{1}{2}}|_{i,j}) - \tfrac{\Delta t}{\Delta y}(H_x^{*n+1}|_{i,j+\frac{1}{2}} - H_x^{*n+1}|_{i,j-\frac{1}{2}}) && \\
& +\tfrac{\Delta t}{\Delta x}(H_y^{*n+1}|_{i+\frac{1}{2},j} - H_y^{*n+1}|_{i-\frac{1}{2},j}) + \tfrac{\Delta t\sigma|_{i,j}}{2}(E_z^{*n+\frac{3}{2}}|_{i,j} + E_z^{*n}|_{i,j}) && = 0
\end{aligned}
$$

and in dispersive media:

$$\begin{array}{ll}
-(H_x^{*n+1}|_{i,j+\frac{1}{2}} - H_x^{*n}|_{i,j+\frac{1}{2}}) - \frac{\Delta t}{\mu|_{i,j+\frac{1}{2}}\Delta y}(E_z^{*n+\frac{1}{2}}|_{i,j+1} - E_z^{*n+\frac{1}{2}}|_{i,j}) & = 0 \\
-(H_y^{*n+1}|_{i+\frac{1}{2},j} - H_y^{*n}|_{i+\frac{1}{2},j}) + \frac{\Delta t}{\mu|_{i+\frac{1}{2},j}\Delta x}(E_z^{*n+\frac{1}{2}}|_{i+1,j} - E_z^{*n+\frac{1}{2}}|_{i,j}) & = 0 \\
-b|_{i,j}(D_z^{*n+\frac{3}{2}}|_{i,j} - D_z^{*n+\frac{1}{2}}|_{i,j}) & \\
+\frac{\Delta t c|_{i,j}}{2}(D_z^{*n+\frac{3}{2}}|_{i,j} + D_z^{*n}|_{i,j}) + \frac{\Delta t\sigma|_{i,j}}{2}(E_z^{*n+\frac{3}{2}}|_{i,j} + E_z^{*n}|_{i,j}) & \\
-\frac{\Delta t}{\Delta y}(H_x^{*n+1}|_{i,j+\frac{1}{2}} - H_x^{*n+1}|_{i,j-\frac{1}{2}}) + \frac{\Delta t}{\Delta x}(H_y^{*n+1}|_{i+\frac{1}{2},j} - H_y^{*n+1}|_{i-\frac{1}{2},j}) & = (E_z - E_z^{obs})|_{i_{obs},j_{obs}}^{n+1} \\
-(E_z^{*n+\frac{3}{2}}|_{i,j} - E_z^{*n+\frac{1}{2}}|_{i,j}) & \\
-a|_{i,j}(D_z^{*n+\frac{3}{2}}|_{i,j} - D_z^{*n+\frac{1}{2}}|_{i,j}) + \frac{\Delta t}{2}(D_z^{*n+\frac{3}{2}}|_{i,j} + D_z^{*n+\frac{1}{2}}|_{i,j}) & = 0
\end{array}$$

4.3.5 Computation of the gradients

Let $\mathbf{U} = \mathbf{U}(\mathbf{p})$ be a solution to the direct state equations. Then the Lagrangian simplifies to:

$$\mathcal{L}(\mathbf{p}, \mathbf{U}(\mathbf{p}), \mathbf{U}^*(\mathbf{p})) = j(\mathbf{p})$$

On the saddle point of the Lagrangian the gradient of $j(p)$ thus become:

$$\frac{\partial j}{\partial p_i} = \frac{d\mathcal{L}}{dp_i} = \frac{\partial \mathbf{U}^T}{\partial p_i}\nabla_{\mathbf{U}}\mathcal{L} + \frac{\partial \mathbf{U}^{*T}}{\partial p_i}\nabla_{\mathbf{U}}^*\mathcal{L} + \frac{\partial \mathcal{L}}{\partial p_i} = \frac{\partial \mathcal{L}}{\partial p_i}$$

The gradients with respect to the material parameters in the non-dispersive case then become:

$$\begin{aligned}
\frac{\partial J}{\partial \mu} &= \int (H_x^* \frac{\partial H_x}{\partial t} + H_y^* \frac{\partial H_y}{\partial t})\, d\Omega \\
\frac{\partial J}{\partial \varepsilon} &= \int E_z^* \frac{\partial E_z}{\partial t}\, d\Omega \\
\frac{\partial J}{\partial \sigma} &= \int E_z^* E_z\, d\Omega
\end{aligned}$$

For the dispersive Debye media the gradients with respect to the material parameters become:

$$\begin{aligned}
\frac{\partial J}{\partial \mu} &= \int \left(H_x^* \frac{\partial H_x}{\partial t} + H_y^* \frac{\partial H_y}{\partial t}\right) dxdydt \\
\frac{\partial J}{\partial \sigma} &= \int E_z^* E_z\, dxdydt \\
\frac{\partial J}{\partial a} &= \int D_z^* \frac{\partial D_z}{\partial t}\, dxdydt \\
\frac{\partial J}{\partial b} &= \int D_z^* \frac{\partial E_z}{\partial t}\, dxdydt \\
\frac{\partial J}{\partial c} &= \int D_z^* E_z\, dxdydt
\end{aligned}$$

The discrete gradients may be formed by simply discretising the continuous gradients using the standard FDTD central differences. The resulting gradient in the non-dispersive case:

$$\begin{aligned}
\frac{\partial J}{\partial \mu} = \sum_{n=1}^{R-1} \sum_{var(\mu)} & \left[H_x^{*n}|_{i,j+\frac{1}{2}} \left(\frac{H_x^{n+\frac{1}{2}}|_{i,j+\frac{1}{2}} - H_x^{n-\frac{1}{2}}|_{i,j+\frac{1}{2}}}{\Delta t} \right) \right. \\
& \left. + H_y^{*n}|_{i+\frac{1}{2},j} \left(\frac{H_y^{n+\frac{1}{2}}|_{i+\frac{1}{2},j} - H_y^{n-\frac{1}{2}}|_{i+\frac{1}{2},j}}{\Delta t} \right) \right] \Delta t \Delta x \Delta y \\
\frac{\partial J}{\partial \varepsilon} = \sum_{n=0}^{R-1} \sum_{var(\varepsilon)} & \left[E_z^{*n+\frac{1}{2}}|_{i,j} \left(\frac{E_z^{n+1}|_{i,j} - E_z^{n}|_{i,j}}{\Delta t} \right) \right] \Delta t \Delta x \Delta y \\
\frac{\partial J}{\partial \sigma} = \sum_{n=0}^{R-1} \sum_{var(\sigma)} & \left[E_z^{*n+\frac{1}{2}}|_{i,j} \left(\frac{E_z^{n+1}|_{i,j} + E_z^{n}|_{i,j}}{2} \right) \right] \Delta t \Delta x \Delta y
\end{aligned}$$

where the notation $var(p)$ means the spatial domain where the parameter p is varied in the optimisation procedure.

In the Debye media the discrete gradient becomes:

$$\frac{\partial J}{\partial \mu} = \sum_{n=1}^{R-1} \sum_{var(\mu)} \left[H_x^{*n}|_{i,j+\frac{1}{2}} \left(\frac{H_x^{n+\frac{1}{2}}|_{i,j+\frac{1}{2}} - H_x^{n-\frac{1}{2}}|_{i,j+\frac{1}{2}}}{\Delta t} \right) + H_y^{*n}|_{i+\frac{1}{2},j} \left(\frac{H_y^{n+\frac{1}{2}}|_{i+\frac{1}{2},j} - H_y^{n-\frac{1}{2}}|_{i+\frac{1}{2},j}}{\Delta t} \right) \right] \Delta t \Delta x \Delta y$$

$$\frac{\partial J}{\partial \sigma} = \sum_{n=0}^{R-1} \sum_{var(\sigma)} \left[E_z^{*n+\frac{1}{2}}|_{i,j} \left(\frac{E_z^{n+1}|_{i,j} + E_z^{n}|_{i,j}}{2} \right) \right] \Delta t \Delta x \Delta y$$

$$\frac{\partial J}{\partial a} = \sum_{n=0}^{R-1} \sum_{var(a)} \left[D_z^{*n+\frac{1}{2}}|_{i,j} \left(\frac{D_z^{n+1}|_{i,j} - D_z^{n}|_{i,j}}{\Delta t} \right) \right] \Delta t \Delta x \Delta y$$

$$\frac{\partial J}{\partial b} = \sum_{n=0}^{R-1} \sum_{var(b)} \left[D_z^{*n+\frac{1}{2}}|_{i,j} \left(\frac{E_z^{n+1}|_{i,j} - E_z^{n}|_{i,j}}{\Delta t} \right) \right] \Delta t \Delta x \Delta y$$

$$\frac{\partial J}{\partial c} = \sum_{n=0}^{R-1} \sum_{var(c)} \left[D_z^{*n+\frac{1}{2}}|_{i,j} \left(\frac{E_z^{n+1}|_{i,j} + E_z^{n}|_{i,j}}{2} \right) \right] \Delta t \Delta x \Delta y$$

We notice that the discrete gradients are summations over the entire time-history of the adjoint and direct fields in the spatial domain where the parameters of interest are varied. To store all these values during the direct and adjoint simulations and then perform the summation may not be feasible in some cases. Fortunately, it is possible to divide the summation at the cost of an extra direct simulation. The technique is illustrated in the figure below:

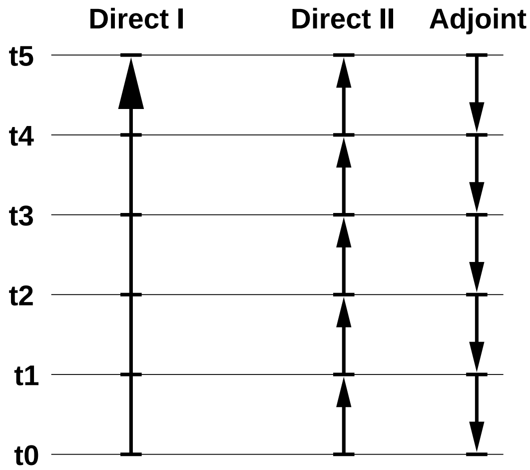

Figure 9: *Memory limited gradient computation*

The figure illustrates how an initial direct simulation is done. During this extra simulation the fields in the entire region are stored at four separate time-steps t_1-t_4. Nothing else is stored during the first direct solution. Then we solve the direct problem again but this time we start at t_4 and store all direct fields in the domain of parameter variation for all time-steps in the interval t_4 to t_5. The next step is to solve the adjoint problem from t_5 to t_4 (backwards in time) and store all adjoint fields in the domain of variation for all time-steps. After this is done we are ready to compute the first contribution to the gradient coming from the time interval t_4 to t_5. This procedure is then carried on for the remaining time-intervals and the contributions are added up to total gradient. The gradient computation in this example requires only 1/5th of the storage usually needed.

5 Optimisation

5.1 Definition of the optimisation problem

Denote by $A : p \longmapsto y = A(p)$ the application (linear or nonlinear forward map) from the space of parameters X into the space of data Y. One also refers to the data y as the image and to p as the object or profile function. The inverse problem consists in solving the operator equation $y = A(p)$ for p, from the knowledge of y. According to the usual definition the inverse problem is well-posed if the three following requirements are fulfilled :

- for every $y \in Y$, a solution p exists.
- the application A is one to one (uniqueness when existence is assumed)
- when p exists then $p = A^{-1}y$ and A^{-1} is a bounded operator (stability of the solution when observed data varies)

A well-known way to find p uses a minimisation procedure (non linear least squares inversion) if X and Y are Hilbert spaces with adapted norms. The problem is written in the following way. Given y in Y and the residual function $f(x) = \|A(x) - y\|^2$, find $p \in K \subset X$ that minimises the residual:

$$f(p) = \min_{q \in K} f(q)$$

Existence and uniqueness are not guaranteed, unless the cost function is convex.

5.2 Unconstrained optimisation

In the table below some of the available methods for unconstrained optimisation are listed. They are categorised by the required derivative information. The algorithms are described in detail in annex **??**.

Required information	Name of method	Comments
$f(p)$	stochastic methods	may be used for the line search problem
$\nabla f(p)$	quasi-Newton, conjugate gradient	requires line search
$\nabla^2 f(p)$	Newton methods	with or without line search

In the IMPACT inverse algorithm the gradient $\nabla f(p)$ is computed at each iteration. Is is consequently possible to use both quasi-Newton and conjugate gradient methods where at each iteration a search direction is generated from the gradient $\nabla f(p)$. The Hessian however is not easily obtained which makes pure Newton methods less suitable.

5.3 The line-search subproblem

In the quasi-Newton and conjugate gradient methods, once a search direction $\mathbf{s}$ has been found, a one-dimensional problem of minimising the cost function along $\mathbf{s}$ is solved to obtain the step length α:

$$\min_{\alpha} f(\alpha)$$

where

$$f(\alpha) = f(\mathbf{p} + \alpha\mathbf{s})$$

A line search algorithm consists of two parts, the bracketing phase and the sectioning/interpolation phase. In the bracketing phase an interval of acceptable values of α is determined. Different criteria for what is an acceptable α value have been suggested, for example the Wolfe-Powell conditions:

$$f(\alpha) \leq f(0) + \alpha\rho f'(0) \;\; \rho \in (0, 0.5)$$

$$|f'(\alpha)| \leq -\sigma f'(0) \;\; \sigma \in (\rho, 1)$$

Typical values of the parameters may be $\rho = 0.01$ and $\sigma = 0.1$ for a fairly accurate line search and $\sigma = 0.9$ for an inexact line search. We notice that the second condition requires that $f'(\alpha)$ is computed.

Once an interval has been found, a more careful search for α is carried out. This may be done by a sectioning method such as golden section or Fibonnaci search or by interpolation or a combination of the two. The interpolation is done by computing the cost function for some points α_i and then fitting to these points a polynomial for which the minima is easy to compute.

In our case, each computation of the cost function means one direct simulation, which implies that an accurate line search will be extremely costly to carry out. It may be necessary to use a very rough line search, for example a quadratic fit of $f(\alpha)$ requiring only one additional direct simulations. For the quasi-Newton method which is known to perform well on inexact line search, this is not a serious matter. The conjugate gradient method on the other hand is more sensitive to the line search and may consequently be a worse choice for our problem.

5.4 Parameter bounds

In most applications there is some a priori knowledge about the values of the parameters. Typically, this information is on the form of bounds on the parameters:

$$a \leq p \leq b$$

In some cases more complicated constraints may be present. It should be possible to treat general linear and nonlinear equality and inequality constraints.

5.5 Tichonov regularisation

5.5.1 Linearisation for sensitivity study

Supposing that $y_0 = A(p_0)$, and linearising around p_0, one obtains

$$\begin{aligned} p &= p_0 + \delta p \\ Y &= y_0 + \delta y \\ A(p) &\approx A(p_0) + A_0'(p_0)\delta p \end{aligned}$$

We obtain the associated linearised minimisation problem

$$j_l(\delta p) = \min_{q \in K} \left(j(q) = \|A_0'(q) - \delta y\|^2 \right) \tag{46}$$

where K is a subset of X

Denote by $\delta p = (A^{+})\delta y$ the solution to (**??**). Existence and uniqueness is not guaranteed. The minimisation procedure shall provide problems if the operator A^{+} is not bounded and if there is noise in information.

5.5.2 Regularisation process

Let R_α be the regularisation operator of A^+ from the space of data Y into the space of parameters X. R_α is a bounded approximation operator of A^+ . The most popular one is the Tichonov regularisation for which R_α is equal to

$$R_\alpha = ({A_0^{'}}^{*} A_0^{'} + \alpha Id)^{-1} {A_0^{'}}^{*}$$

The corresponding non-linear least-squares problem can be regularised, by adding a term to the Lagrangian function as will be seen in the next section. It is well known to improve the condition number and the stability of the solution to the inverse problem . Moreover, convexity of the cost function is better assured.

5.5.3 Stabilising functional

A quite general method for the solution of the inverse problem is based on the so called stabilising functional suggested by Tichonov:

$$\Phi(p) = \frac{1}{2}||u(p) - u_{msr}||^2 + \alpha M(p).$$

M is a smoothing stabilising functional and α a positive number. For instance, a reasonable choice is

$$M(p) = \frac{1}{2}||p - p_0||^2,$$

where the field p_0 is known. We construct a regulariser by solving the following minimisation problem: find $p(\alpha)$ such that $\Phi(p(\alpha)) \leq \Phi(p)$. The strong result is that, under general conditions, a solution to this problem exists and, moreover, with the choice of $M(p)$ given above, this solution is unique. The theory guarantees also the convergence of $p(\alpha)$ to a solution p of $u(p) = u_{msr}$ when $\alpha \to 0$. To solve the regularised problem, one uses various iterative methods. At any step of such an algorithm one solves a well-posed problem, and if this algorithm is convergent, one obtains an approximate solution of the original problem, avoiding expensive minimisation procedures designed for non convex functionals. The most often used minimisation methods make use of gradient methods, which require that one minimises the stabilising functional by iterations.

5.6 Flexibility of the inverse algorithm

The IMPACT algorithm has two main parts, the optimiser and the gradient computation (which includes the direct and adjoint solvers). For flexibility reasons it is desirable that these two parts are kept as separate from each other as possible. We want to be able to choose between different direct/adjoint solvers as well as between different optimisers. The reason we want the optimiser to be exchangeable is that the applicability and efficiency of the optimiser depends on the application (number of parameters, choice of cost function, parameter bounds).

The optimiser and the gradient computation are not always compatible and some interface between the two needs to be defined. Figure **??** illustrates the connecting interface. Observe that ε and μ are just one example of parameters and different applications will have different parameters.

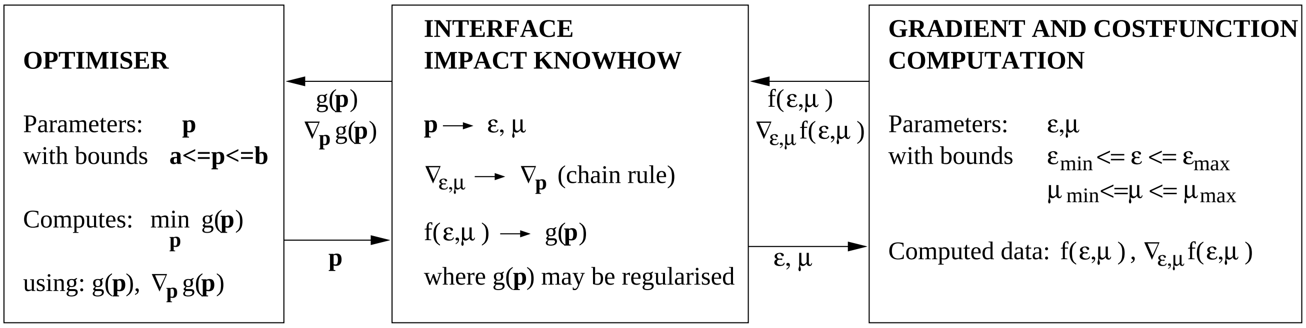

Figure 10: *The interface to the optimiser*

5.6.1 Reverse communication

As pointed out before, the code should be structured in a way that makes it easy to choose between different optimisers and solvers. Necessary modifications of the main program should be kept to a minimum. Recursive communication offers a solution to this problem. A simple example of recursive communication for the inverse algorithm is given below.

```
info = 0
1 continue
call quasiNewton(p,f,dfdp,info)
if info(1)=1
  call costfunction(p,f)
  goto 1
if info(1)=2
  call gradient(p,dfdp)
  goto 1
end if
```

where the vector `info` contains both the number of the task to be performed and the label of the line where `quasiNewton` should procede after the task is finished. Each time a cost function or gradient evaluation is needed in `quasiNewton` the `info` variable is set and a `return` is given. Using this communication model, the different routines needed by the optimiser may easily be exchanged and the modifications in the optimiser code are small.

A Description of the Aerospatiale ACTI3S code

A.1 Acoustic model

A.1.1 The problem

Given an object Ω with boundary Γ embedded in a flood (vacuum most of the time). The flood-structure interaction is solved by the following system:

$$\begin{cases} \Delta u_{diff} + \frac{1}{c^2}\frac{\partial^2 u_{diff}}{\partial t^2} = 0 & \text{in the whole space} \\ \frac{\partial u_{diff}}{\partial n} = -\frac{\partial u_{inc}}{\partial n} & \text{on } \Gamma \end{cases}$$

where u_{diff} is the unknown of the system (scattered pressure) and u_{inc} is a data of the problem (an incident sounding wave for example). The condition on Γ means that the total normal velocity $v = \frac{\partial u_{tot}}{\partial n}$ is equal to zero, as a rigid or inflexible membrane. Speed sound wave propagation in the medium is denoted c ($c = 340 m.s^{-1}$ in the air).

A.1.2 Weak Formulation

In this formulation, g is the data of the problem and $g \in H^3(R^+, H^{-1/2}(\Gamma))$ and we search a function $\Phi \in H^2(R^+, H^{1/2}(\Gamma))$ such that for all Ψ in the same space, we have :

$$\begin{aligned} &\int_R \int_{\Gamma\times\Gamma} \frac{\vec{n}(X).\vec{n}(Y)}{4\pi|X-Y|}\frac{\partial^2\Phi}{\partial t^2}(Y, t - \frac{|X-Y|}{c})\frac{\partial \Psi}{\partial t}(X,t)\ dX dY dt \\ &+c^2 \int_R \int_{\Gamma\times\Gamma} \frac{1}{4\pi|X-Y|} r\vec{o}t_\Gamma \Phi(Y, t - \frac{|X-Y|}{c}) r\vec{o}t_\Gamma \frac{\partial \Psi}{\partial t}(X,t)\ dX dY dt \\ &= \int_R \int_\Gamma g(X,t)\frac{\partial\Psi}{\partial t}(X,t)\ dX dt \end{aligned}$$

A.1.3 Discretization

A.1.3.1 In Time

Basis functions are denoted $\gamma^n(t)$ $(n \geq 1)$ and are defined on the figure **??**.

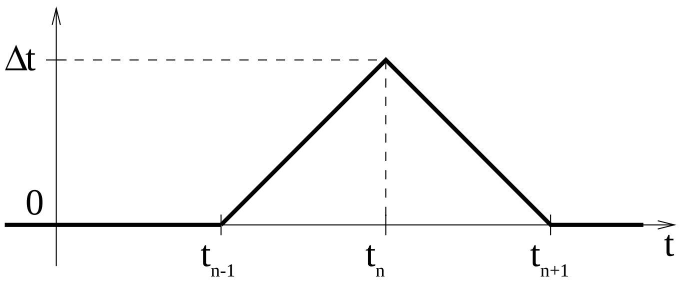

Figure 11: Profile of the function γ_n

We also define the function $\chi_n(t)$ $(n \geq 0)$ whose graph is plotted on the figure **??**.
Then, we have :

$$\begin{aligned} \frac{\partial \gamma_n}{\partial t} &= [\chi_{n-1} - \chi_n] \\ \frac{\partial^2 \gamma_n}{\partial t^2} &= [\delta_{t_{n+1}} - 2\delta_{t_n} + \delta_{t_{n-1}}] \end{aligned}$$

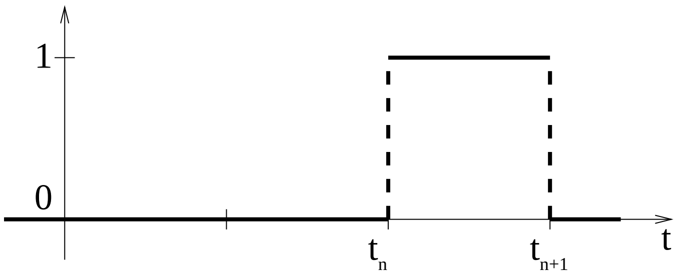

Figure 12: Profile of the function χ_n

A.1.3.2 In space

The equation is solved in space by a surfaciq finite element method. The boundary Γ of the object is meshed with N_h triangular elements. A P1 discretization in space is used. Each basis function φ_i is associated with one vertex S_i, et and is defined by :

$$\begin{cases} \varphi_i(S_j) = 1 \text{ si } i = j \text{ and } 0 \text{ otherwise} \\ \varphi_i \text{ is P1 on each triangle} \end{cases}$$

$\varphi_j(M)$ is the barycentric coordinate of M on the vertex j. Let $\overrightarrow{n_j}$ and $\overrightarrow{t_j}$ respectively the normal and tangent for the edge $[S_j S_{j+1}]$, then we have the expression for φ_j :

$$\varphi_j(M) = \frac{\overrightarrow{S_{j-1}M}.\overrightarrow{n_{j+1}}}{\overrightarrow{S_{j-1}S_j}.\overrightarrow{n_{j+1}}}$$

A.1.3.3 Notation

Let :

$$\Phi(X,t) = \sum_{1 \le j \le N_h} \sum_{m \ge 1} a_j^m \gamma_m(t) \varphi_j(X)$$

and let Ψ , the test function defined by :

$$\frac{\partial \Psi}{\partial t}(X,t) = \chi_{n-1}(t)\varphi_i(X)$$

A.1.4 Linear system

Let A^m be the solution vector at the date t^m : $A^m = [a_j^m]_{1 \le j \le N_h}$. For each time step t^n $(n \ge 1)$ the following linear system is solved :

$$\sum_{m=\sup(1,n-2-L/\Delta t)}^{n} M^{n-m}.A^m = B^n$$

and the right hand side is:

$$B_i^n = \int_{t_{n-1} \le t \le t_n} \int_\Gamma g(X,t).\varphi_i(X)\ dX dt$$

with the matrix M^k :

$$\begin{aligned} M_{ij}^k \quad = \quad & \int_{\Gamma \times \Gamma} \frac{\vec{n}(X).\vec{n}(Y)}{4\pi|X-Y|} \varphi_i(X)\varphi_j(Y) \\ & \left[\chi^0(\frac{|X-Y|}{c} - t_k) - 2\chi^0(\frac{|X-Y|}{c} - t_{k-1}) + \chi^0(\frac{|X-Y|}{c} - t_{k-2})\right] \ dX dY dt \\ & + c^2 \int_0^{\Delta t} \int_{\Gamma\times\Gamma} \frac{\vec{rot}\varphi_i(X)\vec{rot}\varphi_j(Y)}{4\pi|X-Y|} \gamma_1(t + t_k - \frac{|X-Y|}{c})\ dX dY dt \end{aligned}$$

For example, with n=3, the system becomes :

$$M^2.A^1 + M^1.A^2 + M^0.A^3 = B^3$$

where the only unknown is A^3.
We clearly see three contributions in the system :

- The term B^n is representative of the excitation (or other data) ;
- The term $\sum_{1\leq m\leq n-1} M^{n-m}.A^m$ is representative of the past contribution ;
- The term $M^0.A^n$ is the present contribution, to compute

Physically, the expression of this equation is explained by the fact that what occurs at the date n (*i.e.* A^n) is a consequence of what occured at the date $(n-m)$ on the elements situated at a distance $m.c.\Delta t$ (*i.e.* A^{n-m}) for all $n > 1$. Mathematically, this causality link is contained in the expression of the matrices M^k. Indeed, M^k is representative of the interactions between elements situated at a distance $k.c.\Delta t$ each other. Therefore :

- (M^k) are sparse (for a given element e_1, the elements e_2 situated at a distance $k.c.\Delta t$ from e_1 do not constitute an important portion of the mesh) ;
- M^0 is almost diagonal (because it only takes account the self-interaction of elements or eventually with their nearby neighbours;
- The (M^k) have an aspect plotted on the figure **??**.

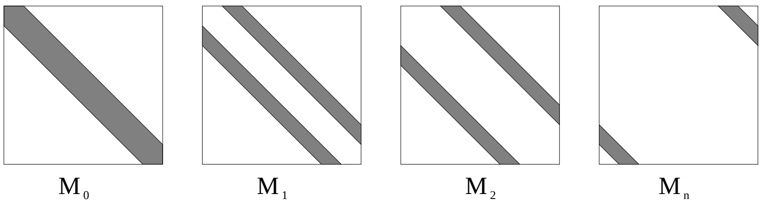

Figure 13: Aspect of the matrices M^k

A.1.5 Matrices M^k

The matrices M^k can be developped in the following expressions:

$$\begin{aligned}
M_{ij}^k = & \int\int_{t_k\leq\frac{|X-Y|}{c}\leq t_{k+1}} \frac{\vec{n}(X).\vec{n}(Y)}{4\pi|X-Y|}\varphi_i(X)\varphi_j(Y)dXdY \\
& -2\int\int_{t_{k-1}\leq\frac{|X-Y|}{c}\leq t_k} \frac{\vec{n}(X).\vec{n}(Y)}{4\pi|X-Y|}\varphi_i(X)\varphi_j(Y)dXdY \\
& +\int\int_{t_{k-2}\leq\frac{|X-Y|}{c}\leq t_{k-1}} \frac{\vec{n}(X).\vec{n}(Y)}{4\pi|X-Y|}\varphi_i(X)\varphi_j(Y)dXdY \\
& +\int\int_{t_k\leq\frac{|X-Y|}{c}\leq t_{k+1}} \frac{\vec{rot}\varphi_i(X)\vec{rot}\varphi_j(Y)}{4\pi|X-Y|}\frac{1}{2}(c.t_k-|X-Y|+c.\Delta t)^2 \\
& +\int\int_{t_{k-1}\leq\frac{|X-Y|}{c}\leq t_k} \frac{\vec{rot}\varphi_i(X)\vec{rot}\varphi_j(Y)}{4\pi|X-Y|}\frac{1}{2}(c^2.\Delta t^2-2(c.t_k-|X-Y|)^2+2c.\Delta t(c.t_k-|X-Y|)) \\
& +\int\int_{t_{k-2}\leq\frac{|X-Y|}{c}\leq t_{k-1}} \frac{\vec{rot}\varphi_i(X)\vec{rot}\varphi_j(Y)}{4\pi|X-Y|}\frac{1}{2}(c.t_k-|X-Y|-2c.\Delta t)^2
\end{aligned}$$

A.1.6 Exterior pressure computation

Denote by G the 3D time domain Green function

$$G(x,t) = \frac{1}{4\pi}\frac{\delta\left(t-|x|\right)}{|x|}$$

Define the integral double layer operator K, for Φ a regular function defined on Γ (solution of the variationnal equation above and with time domain representation X^m), and for an exterior point x by :

$$L\Phi(x,t) = \int_R \int_\Gamma \frac{\partial G}{\partial n_y}(x-y, t-\tau)\Phi(y,\tau)d\Gamma_y d\tau$$

Then the exterior acoustic near field acoustic pressure can be computed by :

$$u = L[u]$$

where $[u]$ is the solution of the integral equation (weak formulation above).
For the far field, one has the expression :

$$u_{far}(t) = \frac{1}{4\pi rc}\int_\Gamma \frac{\partial}{\partial t}\Phi(y, t - \frac{\overrightarrow{OY}.\vec{u}}{c})d\Gamma_y$$

The quantity $t - \frac{\overrightarrow{OY}.\vec{u}}{c}$ is representative of the delay time for the wave to go from the point Y to the point of far field.
For the computation of near field and far field, Gauss points are used. For very near field computations, with very low distances (the order of $lambda$) from the object surface, more Gauss points will be used.

A.2 Excitations

The code can treat two kind of excitations :

sinusoidal excitation : $s(t) = sin(\omega.t)$

gaussian excitation : $s(t)$ can be written :

$$s(t) = exp(-\pi\left(\frac{ct - \frac{c}{f}\sqrt{-\frac{log\alpha}{\pi}}\sqrt{-\frac{logD}{\pi}}}{\frac{c}{f}\sqrt{-\frac{log\alpha}{\pi}}}\right)^2)$$

f is the maximum propagating frequency. D and $s(0)$ represents the discontinuity at $t=0$.
Finally, α is the FFT value of the function $s()$ at the frequency f. Most of the time $\alpha = 0,1$ and $D = 0,01$.

A.3 Functionnalities

The delayed time potential code can take account the action of the plane wave and generators on sound hard structure meshed by triangles. It works with sinusoidal or gaussian excitation. It does not take account spherical wave, crenel or square-sinus excitation.

B Description of the CRS4 MOD3D code

B.1 Summary

MOD3D: a compact finite difference code to model the 3D scalar acoustic wave propagation in an isotropic, inhomogeneous medium, emitted from an arbitrary source geometry. This code was originally exploited to produce synthetic seismic traces and, in its reverse time version, to invert seismic data. Time integration is achieved through a fourth-order five-step leap-frog scheme. The scheme is time-reversible and permits direct access to the time derivative of the field, useful for monitoring the energy flow. The Laplacian evaluation is performed using a sixth-order implicit scheme, allowing spectral-like accuracy. A detailed characterization of dispersion permits the optimization of time and space discretization intervals. Formulating the 3D acoustic wave equation in Hamiltonian form yields direct access to the generalized field momentum, making it possible to monitor local energy flux directly and locally impose a direction on this flux. This provides a way to tweak the energy near the boundary and implement good absorbing boundary conditions using only the lowest-order paraxial equation. The actual numerical energy, and not a discretization of the continuous energy, is monitored; trapping width is optimized with respect to a reflectivity threshold. The overall method is well-posed (both by energy and mode analysis criteria), parallel and high-quality.

B.2 Propagation model

Wave Propagation modelling is based on the solution of the acoustic wave equation, forward in time in the finite volume Ω:

$$\left[\partial_{tt} - c^2\left(x,y,z\right)\nabla^2\right] P\left(x,y,z,t\right) = 0 \quad t \in [0,T) \quad (x,y,z) \in \Omega \tag{47}$$

Time marching proceeds from time zero with initial conditions

$$P\left(x,y,z,t=0)\right) = P_0\left(x,y,z\right), \quad \dot{P}\left(x,y,z,t=0\right) = Q_0\left(x,y,z\right), \tag{48}$$

up to time T. The introduction of a finite volume Ω is necessary because the numerical solution requires a finite computational bulk. Artificial absorbing boundary conditions (ABC) are then imposed, to simulate an outflowing propagation:

$$\mathcal{B}\left(\partial_x, \partial_y, \partial_z, \partial_t\right) P(x,y,z,t) = 0 \quad (x,y,z) \in \partial\Omega. \tag{49}$$

$\mathcal{B}$ represents the one-way boundary operator. The numerical implementation of Eqns.(**??**-**??**) involves the following choices: the time integrator (Sec. **??**), the Laplacian approximation (Sec. **??**), the ABC operator $\mathcal{B}$ and its discretization scheme.

B.3 Numerical implementation

Eqn.(**??**) must be approximated in space and time. The choice of a particular scheme is based on the trade–off between accuracy and computational cost. Numerical stability and dispersion impose strong constraints on discretization parameters $\Delta x, \Delta y, \Delta z, \Delta t$. We have used the maximum admissible stepsizes in space and time, as a major criterion in the evaluation of different schemes. The larger the admissible stepsizes, the less costly the modelling – in memory and CPU time. This criterion led to the following choice.

B.3.1 Time integration

We introduce the time discretization $t_n = n\Delta t$, defining as usual $P^{(n)}(x,y,z) = P(x,y,z,t_n)$. Starting from the Hamiltonian form of the wave equation (**??**),

$$\left\{ \begin{array}{rcl} \dot{P} & = & Q \\ \dot{Q} & = & c^2\nabla^2 P, \end{array} \right. \tag{50}$$

one can integrate using the leap scheme (we omitted for clarity x, y, z):

$$\begin{cases} Q^{(n+\frac{1}{3})} & = & Q^{(n)} & + & \frac{1}{6}\,\Delta t c^2 \nabla^2 P^{(n)} \\ P^{(n+\frac{1}{2})} & = & P^{(n)} & + & \frac{1}{2}\,\Delta t Q^{(n+\frac{1}{3})} \\ Q^{(n+\frac{2}{3})} & = & Q^{(n+\frac{1}{3})} & + & \frac{2}{3}\,\Delta t c^2 \nabla^2 P^{(n+\frac{1}{2})} \\ P^{(n+1)} & = & P^{(n+\frac{1}{2})} & + & \frac{1}{2}\,\Delta t Q^{(n+\frac{2}{3})} \\ Q^{(n+1)} & = & Q^{(n+\frac{2}{3})} & + & \frac{1}{6}\,\Delta t c^2 \nabla^2 P^{(n+1)} \end{cases} \tag{51}$$

Without any increase in memory requirements over the standard central finite difference integration scheme, using Eqns.(**??**) we obtain a fourth order accuracy in P. This integration scheme gives direct acces to the field time derivative Q (the generalized momentum), that will be useful for implementing the absorbing boundary conditions. Remark that Eqns.(**??**) preserve the time-reversal symmetry of the wave equation and, furthermore, the Jacobian of the mapping that they define is one. Both properties are consistent with the characteristic of a Hamiltonian system.

B.3.2 Laplacian approximation

From Eqns.(**??**), we observe that the scheme requires twice at each integration step the evaluation of the Laplacian of P on each point $(x, y, z) \in \Omega$. For this purpose, Ω, a cube in our applications, is regularly meshed, $x_i = (i-1)\Delta x$, $y_j = (j-1)\Delta y$, $z_k = (k-1)\Delta z$, where $i = 1, 2, \ldots, N_x$, $j = 1, 2, \ldots, N_y$ and $k = 1, 2, \ldots, N_z$, allowing the evaluation of P on the grid, $P_{ijk}(t) = P(x_i, y_j, z_k, t)$. In standard central finite differences, second derivatives at each mesh point are approximated explicitely from the values of P at neighboring points. In the spectral approach, on the other hand, each second derivative is computed in the Fourier space multiplying the transformed field $\hat{P}$ by the squared wave number. This corresponds in the direct space to a convolution, and then to a contribution from all the nodes along the selected direction. One can attempt to mimic this last property in the direct space, by writing a global dependency of the second derivative from all values of P along a principal direction in the lattice. This idea is behind the concept of compact finite differencies, in which the approximation of second derivatives, requiring sixth order accuracy at a small computational cost, leads to a system of linear equations. For instance along the x-axis, omitting for clarity t, j and k this system is written as follows:

$$2P''_{i+1} + 11P''_i + 2P''_{i-1} = \frac{3}{4}\left(P_{i+2} - 2P_i + P_{i-2}\right) + 12\left(P_{i+1} - 2P_i + P_{i-1}\right), \tag{52}$$

where $i = 3, 4, \ldots, N_x - 3$. Near the boundaries, $i = 2$ and $i = N_x - 1$, we impose a similar closure condition to obtain globally a tridiagonal system of equations:

$$P''_{i-1} + 10P''_i + P''_{i+1} = 12\left(P_{i-1} - 2P_i + P_{i+1}\right), \tag{53}$$

with $P''_1 = 0$ and $P''_{N_x} = 0$. Representing the solution of Eqns. (**??**) and (**??**) in the matrix-vector form where $\mathbf{T}$ and $\mathbf{R}$ are, respectively, tridiagonal and pentadiagonal matricess,

$$\vec{P}'' = \mathbf{T}^{-1}\mathbf{R}\vec{P}, \tag{54}$$

we perceive clearly the globalness of the method, being the inverse of $\mathbf{T}$ a dense matrix.

B.4 Absorbing Boundary Condition

B.4.1 Part I: Absorbing Boundary Equations

Simulation of wave propagation is usually restricted to a small portion of the physical space. Arificial boundary conditions are required where the model is truncated in space. Absorbing boundaries should ensure that waves impinging the artificial boundaries are not reflected. Our approach is to solve the lowest order approximation of the one-way scalar wave equation. For instance, at the left boundary $(x = 0, y, z)$, the outflowing wave is driven by:

$$\left(\partial_t - c\,\partial_x\right) P = 0. \tag{55}$$

A simple analysis of the reflection properties of such a boundary provides the following reflection coefficient:

$$R = \frac{1 - \cos\theta}{1 + \cos\theta} \tag{56}$$

where $\theta \in [0, \pi/2]$ is the angle between the normal to the boundary and the wavevector $\vec{k}$: $\cos\theta = k_x/|\vec{k}|$. From Eqn. (**??**), we see that a normal incident wave is perfeclty absorbed, $(R = 0)$. The reflection coefficient R tends to one when θ goes to $\pi/2$. Eqn.(**??**) is approximated in the simplest way, using forward finite differences on nodes $i = 1$ and 2 (indexes j and k were omitted for clarity):

$$P_i^{(n+1)} - P_i^{(n)} - c\frac{\Delta t}{\Delta x}\left(P_{i+1}^{(n)} - P_i^{(n)}\right) = 0. \tag{57}$$

Similarly, for $i = N_x$ and $N_x - 1$, we write

$$P_i^{(n+1)} - P_i^{(n)} + c\frac{\Delta t}{\Delta x}\left(P_i^{(n)} - P_{i-1}^{(n)}\right) = 0. \tag{58}$$

B.4.2 Part II: Energy flow and Q reversal

From Eqn.(**??**) it is possible to derive the energy contained inside a bounded domain Ω, a function of time t, and evaluate its derivative:

$$H(t) = \frac{1}{2}\int_\Omega \left[(\nabla P)^2 + \left(\frac{Q}{c}\right)^2\right] dV \Rightarrow \frac{dH}{dt} = \int_{\partial\Omega} Q\,\vec{\nabla}P \cdot d\vec{\sigma}. \tag{59}$$

$\vec{J} = Q\vec{\nabla}P$ represents the local energy flux density through the boundaries. If $\vec{J} \cdot d\vec{\sigma}$ vanishes on the boundary, the energy H is conserved. Where $\vec{J}$ points outward, the energy flows in, viceversa, where $\vec{J}$ points inward, the energy flows out. Then, our strategy for constraining all waves to flow out of the computational bulk, is to locally revert the sign of Q in each point of the boundaries where the projection of $\vec{J}$ along the normal $\hat{n}$ is positive:

$$\forall(x, y, z) \in \partial\Omega \;\; \text{WHERE} \;\; \vec{J} \cdot \hat{n} > 0 \Rightarrow Q(x, y, z) \to -Q(x, y, z) \tag{60}$$

This technique can be easily applied, provided the scheme permits a direct acces to Q, as the Hamiltonian approach does.

B.4.3 Numerical Implementation of the complete algorithm

In the numerical implementation, the preceding technique can be used, provided that the zone where the Q reversal is applied, is enlarged to a thin layer all around the inner bulk. In this way, as the numerical experiments confirm, the energy is trapped in a strip pattern inside this layer. To dissipate this unwanted energy, source of numerical errors, we adopt the simplest absorbing equation, namely Eqn.(**??**).

C Description of the KTH pscyee2d code

C.1 The Maxwell equations

The time-dependent electromagnetic field is governed by the Maxwell equations. In differential form they are written as:

$$-\frac{\partial \mathbf{B}}{\partial t} = \nabla \times \mathbf{E} \tag{61}$$

$$\frac{\partial \mathbf{D}}{\partial t} = \nabla \times \mathbf{H} - \mathbf{J} \tag{62}$$

$$\nabla \cdot \mathbf{D} = \rho \tag{63}$$

$$\nabla \cdot \mathbf{B} = 0 \tag{64}$$

where $\mathbf{E}$ is the electric field in V/m, $\mathbf{D}$ the electric flux density in C/m^2, $\mathbf{H}$ the magnetic field in A/m, $\mathbf{B}$ the magnetic flux density in Vs/m^2, $\mathbf{J}$ the electric current density in A/m^2 and ρ the charge density in C/m^3.

In linear, isotropic and non-dispersive media the constitutive relations are:

$$\begin{aligned}\mathbf{B} &= \mu\mathbf{H}\\ \mathbf{D} &= \varepsilon\mathbf{E}\\ \mathbf{J} &= \sigma\mathbf{E}.\end{aligned}$$

where the permittivity ε, the permeability μ and the conductivity σ are constant in time. Substituting the constitutive relations into equations (**??**) and (**??**) results in:

$$-\mu\frac{\partial \mathbf{H}}{\partial t} = \nabla \times \mathbf{E} \tag{65}$$

$$\varepsilon\frac{\partial \mathbf{E}}{\partial t} = \nabla \times \mathbf{H} - \sigma\mathbf{E} \tag{66}$$

The divergence equations (**??**) and (**??**) follow from the curl equations and need not be solved explicitly in the algorithm. However, it is necessary that the discrete fields satisfy the divergence equations to avoid generating spurious charge. This property is inherent in the staggered grid discretization used in FDTD.

In Cartesian coordinates equations (**??**) and (**??**) may be written as a system of six coupled scalar PDEs for the unknowns E_x, E_y, E_z, H_x, H_y and H_z:

$$\mu\frac{\partial H_x}{\partial t} = \frac{\partial E_y}{\partial z} - \frac{\partial E_z}{\partial y} \tag{67}$$

$$\mu\frac{\partial H_y}{\partial t} = \frac{\partial E_z}{\partial x} - \frac{\partial E_x}{\partial z} \tag{68}$$

$$\mu\frac{\partial H_z}{\partial t} = \frac{\partial E_x}{\partial y} - \frac{\partial E_y}{\partial x} \tag{69}$$

$$\varepsilon\frac{\partial E_x}{\partial t} = \frac{\partial H_z}{\partial y} - \frac{\partial H_y}{\partial z} - \sigma E_x \tag{70}$$

$$\varepsilon\frac{\partial E_y}{\partial t} = \frac{\partial H_x}{\partial z} - \frac{\partial H_z}{\partial x} - \sigma E_y \tag{71}$$

$$\varepsilon\frac{\partial E_z}{\partial t} = \frac{\partial H_y}{\partial x} - \frac{\partial H_x}{\partial y} - \sigma E_z \tag{72}$$

In two dimensions the above system decouples into two systems. The TM (transverse magnetic) mode:

$$\mu \frac{\partial H_x}{\partial t} = -\frac{\partial E_z}{\partial y} \tag{73}$$

$$\mu \frac{\partial H_y}{\partial t} = \frac{\partial E_z}{\partial x} \tag{74}$$

$$\varepsilon \frac{\partial E_z}{\partial t} = \frac{\partial H_y}{\partial x} - \frac{\partial H_x}{\partial y} - \sigma E_z \tag{75}$$

and the TE (transverse electric) mode:

$$\varepsilon \frac{\partial E_x}{\partial t} = \frac{\partial H_z}{\partial y} - \sigma E_x$$

$$\varepsilon \frac{\partial E_y}{\partial t} = -\frac{\partial H_z}{\partial x} - \sigma E_y$$

$$\mu \frac{\partial H_z}{\partial t} = \frac{\partial E_x}{\partial y} - \frac{\partial E_y}{\partial x}$$

C.2 The Yee scheme

The following algorithm was introduced by Kane S. Yee in 1966 [?]. For a thorough description of FDTD see [?].

The spatial discretization used in FDTD is a uniform, Cartesian grid where the electric and magnetic fields are staggered. The three-dimensional grid is best described by studying the unit cell:

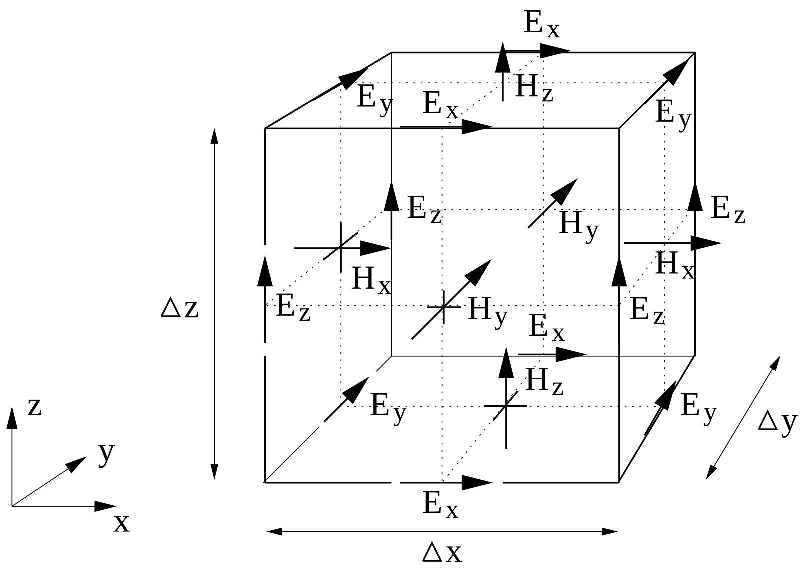

Figure 14: *The Yee unit cell.*

As illustrated the electric fields are located on the midpoint of the cell edges and the magnetic fields are located at the center of the cell faces. The grid is indexed using the convention that index (i, j, k) corresponds to the physical coordinates $(i\Delta x, j\Delta y, k\Delta z)$. Half increments (and decrements) of the indices are used to denote the midpoints between cell corners. The staggered grid in two dimensions (TM case) is illustrated in the figure below:

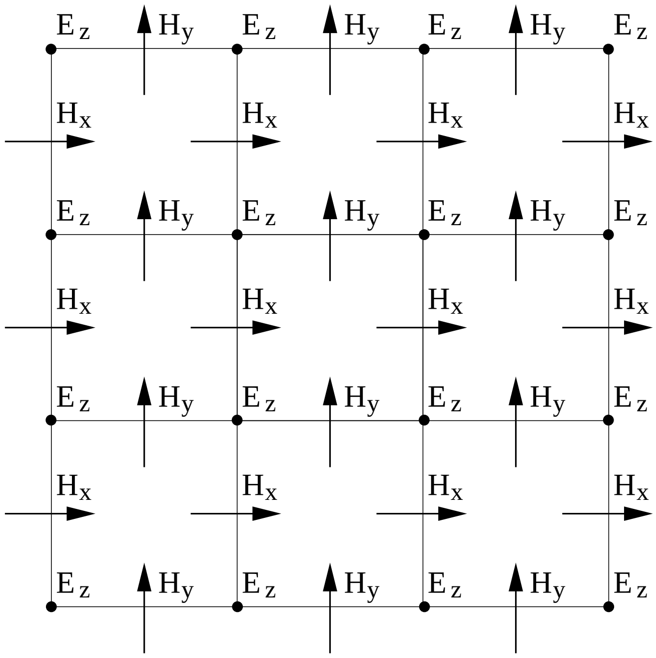

Figure 15: *Staggered grid in 2D (TM).*

The discretization in time uses the second order accurate leapfrog scheme with the electric and magnetic fields staggered one half time-step. The electric fields are located at time-levels corresponding to whole increments of Δt and the magnetic fields at half increments. Using central finite differences for the space derivatives the time-stepping expressions may be formed. In two dimensions (TM) the full set of time-stepping expressions become (compare with (**??**)-(**??**)):

$$H_x|_{i,j+\frac{1}{2}}^{n+\frac{1}{2}} = H_x|_{i,j+\frac{1}{2}}^{n-\frac{1}{2}} - \frac{\Delta t}{\mu}\left[\frac{E_z|_{i,j+1}^{n} - E_z|_{i,j}^{n}}{\Delta y}\right]$$

$$H_y|_{i+\frac{1}{2},j}^{n+\frac{1}{2}} = H_y|_{i+\frac{1}{2},j}^{n-\frac{1}{2}} + \frac{\Delta t}{\mu}\left[\frac{E_z|_{i+1,j}^{n} - E_z|_{i,j}^{n}}{\Delta x}\right]$$

$$E_z|_{i,j}^{n+1} = \left(\frac{1-\frac{\sigma\Delta t}{2\varepsilon}}{1+\frac{\sigma\Delta t}{2\varepsilon}}\right) E_z|_{i,j}^{n} + \left(\frac{\frac{\Delta t}{\varepsilon}}{1+\frac{\sigma\Delta t}{2\varepsilon}}\right)\left[\frac{H_y|_{i+\frac{1}{2},j}^{n+\frac{1}{2}} - H_y|_{i-\frac{1}{2},j}^{n+\frac{1}{2}}}{\Delta x} - \frac{H_x|_{i,j+\frac{1}{2}}^{n+\frac{1}{2}} - H_x|_{i,j-\frac{1}{2}}^{n+\frac{1}{2}}}{\Delta y}\right]$$

Notice that a semi-implicit time average has been used for the electric field on the right-hand side of equation (**??**). This is necessary since in the discretized equation this field is centered between the time-levels $n+1$ and n used in the central difference approximation of the time-derivative.

$$E_z|_{i,j}^{n+\frac{1}{2}} \approx \frac{E_z|_{i,j}^{n+1} + E_z|_{i,j}^{n}}{2} \tag{76}$$

The stability criterion for the Yee-sheme in two dimensions is (CFL):

$$\Delta t \leq \frac{1}{c\sqrt{\frac{1}{(\Delta x)^2} + \frac{1}{(\Delta y)^2}}} \tag{77}$$

C.3 Incident fields and sources

Two different types of excitations are used, point source and plane wave. The point source is modeled by simply adding a source term to the correct electric field component after the usual update:

$$E = E + E_{source}$$

An alternative way of modeling the point source is using a hard source:

$$E = E_{source}$$

where the field is forced to the excitation function. However, this type of source has limited use due to the fact that while the additative source is transparent to incoming waves the hard source acts as a reflector. In most scattering problems reflections will eventually travel back to the location of the source in which case the hard source is not suitable.

Plane waves are modeled by radiating boundaries, or Huygens surfaces [**?**]. This approach is based on the linearity of Maxwell's equations and the decomposition of the fields as:

$$E^{tot} = E^{inc} + E^{sca}$$
$$H^{tot} = H^{inc} + H^{sca}$$

where E^{inc} and H^{inc} are assumed to be known in all space for all times. The computational domain is separated into a total field zone and a scattered field zone as illustrated in figure **??**.

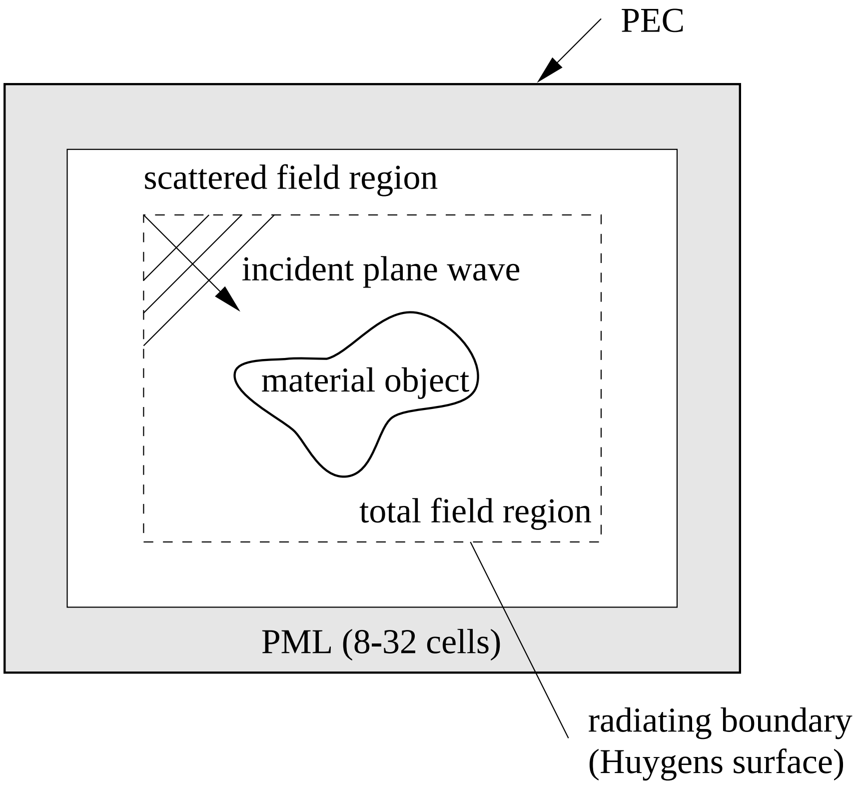

Figure 16: *Computational domain in 2D FDTD.*

The boundary separating the two regions is typically placed a few cells from the border to avoid interfering with ABCs and at the same time avoid limiting the total field zone more than necessary. In the total field zone the Maxwell equations work on total field quantities and in the scattered field zone on the scattered fields. The excitation may then be implemented by modifying the time-stepping expressions for the field components with stencils in both zones, i.e. only cells on the boundary between the total and scattered field regions are affected.

C.4 Absorbing boundary conditions, ABC

Two different absorbing boundary conditions are implemented in the code, first order Mur [?] (used for validation purposes) and uniaxial perfectly matched layer, UPML [?]. UPML is a variant of the original PML formulation [?] based directly on the Maxwell equations.

The Mur ABC is effectively a finite difference implementation of an ABC developed by Engquist and Majda based on the factorization of the wave equation operator [?]. At the $x = 0$ boundary in a two-dimensional grid the first order Engquist-Majda absorbing boundary condition for E_z is:

$$\frac{\partial E_z}{\partial x} - \frac{1}{c_0}\frac{\partial E_z}{\partial t} = 0$$

Approximating the partial derivatives with central finite differences around an auxiliary point $E_z(\frac{1}{2}, j)$ results in the following time-stepping expression for the E_z field on the boundary:

$$E_z^{n+1}|_{0,j} = E_z^n|_{1,j} + \frac{c_0\Delta t - \Delta x}{c_0\Delta t + \Delta x}(E_z^{n+1}|_{1,j} - E_z^n|_{0,j})$$

The UPML ABC is based on the fact that for a plane wave incident on a uniaxial media it is possible to derive conditions for the permittivity and permeability such that the wave will be purely transmitted into the media. The idea is to surround the computational domain with a highly lossy layer of such media terminated by a PEC (perfect electric conductor) wall as illustrated in figure **??**.

The Maxwell equations in a uniaxial media are:

$$\nabla \times \mathbf{H} = j\omega\varepsilon_0\overline{\overline{\varepsilon}}\mathbf{E} \tag{78}$$

$$\nabla \times \mathbf{E} = -j\omega\mu_0\overline{\overline{\mu}}\mathbf{H} \tag{79}$$

The reflectionless condition for $\overline{\overline{\varepsilon}}$ and $\overline{\overline{\mu}}$ in the two dimensional TM case is:

$$\overline{\overline{\varepsilon}} = \begin{bmatrix} \frac{s_y}{s_x} & 0 & 0 \\ 0 & \frac{s_x}{s_y} & 0 \\ 0 & 0 & s_x s_y \end{bmatrix} \text{ and } \overline{\overline{\mu}} = \begin{bmatrix} \frac{s_y}{s_x} & 0 & 0 \\ 0 & \frac{s_x}{s_y} & 0 \\ 0 & 0 & s_x s_y \end{bmatrix} \tag{80}$$

where s_x corresponds to the uniaxial layer normal to the x-axis and s_y to the layer normal to the y-axis. They are typically chosen as:

$$\begin{aligned} s_x &= 1 + \frac{\sigma_x}{j\omega\varepsilon_0} \\ s_y &= 1 + \frac{\sigma_y}{j\omega\varepsilon_0} \end{aligned}$$

in order to introduce loss. Due to the dispersive properties of the chosen permittivity and permeability tensors the time-domain Maxwell equations have to be solved in a two step procedure. We introduce the magnetic and electric flux vectors:

$$\begin{aligned} \mathbf{B}_x &= \frac{1}{s_x}\mathbf{H}_x \\ \mathbf{B}_y &= \frac{1}{s_x}\mathbf{H}_y \\ \mathbf{D}_z &= s_y\mathbf{E}_z \end{aligned}$$

and Fourier transform the Maxwell equations (**??**) and (**??**) into the time-domain to obtain:

$$\begin{aligned}
\frac{\partial B_x}{\partial t} + \frac{\sigma_y}{\epsilon_0}B_x + \frac{1}{\mu_0}\frac{\partial E_z}{\partial y} &= 0 \\
\frac{\partial B_x}{\partial t} + \frac{\sigma_x}{\epsilon_0}B_x - \frac{\partial H_x}{\partial t} &= 0 \\
\frac{\partial B_y}{\partial t} + \frac{\sigma_x}{\epsilon_0}B_y - \frac{1}{\mu_0}\frac{\partial E_z}{\partial x} &= 0 \\
\frac{\partial B_y}{\partial t} + \frac{\sigma_y}{\epsilon_0}B_y - \frac{\partial H_y}{\partial t} &= 0 \\
\frac{\partial D_z}{\partial t} + \frac{\sigma_x}{\epsilon_0}D_z + \frac{1}{\epsilon_0}\left(\frac{\partial H_x}{\partial y} - \frac{\partial H_y}{\partial x}\right) &= 0 \\
\frac{\partial D_z}{\partial t} - \frac{\partial E_z}{\partial t} - \frac{\sigma_y}{\epsilon_0}E_z &= 0
\end{aligned}$$

These equations may be numerically realized in the Yee grid by using standard central differences for the partial derivatives. The resulting time-stepping expressions become:

$$\begin{aligned}
B_x^{n+\frac{1}{2}}|_{i,j+\frac{1}{2}} = \; & \frac{2\varepsilon_0-\Delta t\sigma_y|_{i,j+\frac{1}{2}}}{2\varepsilon_0+\Delta t\sigma_y|_{i,j+\frac{1}{2}}} B_x^{n-\frac{1}{2}}|_{i,j+\frac{1}{2}} \\
& -\frac{2\varepsilon_0}{2\varepsilon_0+\Delta t\sigma_y|_{i,j+\frac{1}{2}}}\frac{\Delta t}{\mu_0\Delta y}\left(E_z^n|_{i,j+1}-E_z^n|_{i,j}\right) \\
H_x^{n+\frac{1}{2}}|_{i,j+\frac{1}{2}} = \; & H_x^{n-\frac{1}{2}}|_{i,j+\frac{1}{2}} \\
& +\frac{\Delta t\sigma_x|_{i,j+\frac{1}{2}}}{2\varepsilon_0}\left(B_x^{n+\frac{1}{2}}|_{i,j+\frac{1}{2}}+B_x^{n-\frac{1}{2}}|_{i,j+\frac{1}{2}}\right) \\
& +\left(B_x^{n+\frac{1}{2}}|_{i,j+\frac{1}{2}}-B_x^{n-\frac{1}{2}}|_{i,j+\frac{1}{2}}\right) \\
B_y^{n+\frac{1}{2}}|_{i+\frac{1}{2},j} = \; & \frac{2\varepsilon_0-\Delta t\sigma_x|_{i+\frac{1}{2},j}}{2\varepsilon_0+\Delta t\sigma_x|_{i+\frac{1}{2},j}} B_y^{n-\frac{1}{2}}|_{i+\frac{1}{2},j} \\
& +\frac{2\varepsilon_0}{2\varepsilon_0+\Delta t\sigma_x|_{i+\frac{1}{2},j}}\frac{\Delta t}{\mu_0\Delta x}\left(E_z^n|_{i+1,j}-E_z^n|_{i,j}\right) \\
H_y^{n+\frac{1}{2}}|_{i+\frac{1}{2},j} = \; & H_y^{n-\frac{1}{2}}|_{i+\frac{1}{2},j} \\
& +\frac{\Delta t\sigma_x|_{i+\frac{1}{2},j}}{2\varepsilon_0}\left(B_y^{n+\frac{1}{2}}|_{i+\frac{1}{2},j}+B_y^{n-\frac{1}{2}}|_{i+\frac{1}{2},j}\right) \\
& +\left(B_y^{n+\frac{1}{2}}|_{i+\frac{1}{2},j}-B_y^{n-\frac{1}{2}}|_{i+\frac{1}{2},j}\right) \\
D_z^{n+1}|_{i,j} = \; & \frac{2\varepsilon_0-\Delta t\sigma_x|_{i,j}}{2\varepsilon_0+\Delta t\sigma_x|_{i,j}} D_z^n|_{i,j} \\
& +\frac{2\Delta t}{2\varepsilon_0+\Delta t\sigma_x|_{i,j}}\left(\frac{H_y^{n+\frac{1}{2}}|_{i+\frac{1}{2},j}-H_y^{n+\frac{1}{2}}|_{i-\frac{1}{2},j}}{\Delta x}-\frac{H_x^{n+\frac{1}{2}}|_{i,j+\frac{1}{2}}-H_x^{n+\frac{1}{2}}|_{i,j-\frac{1}{2}}}{\Delta y}\right) \\
E_z^{n+1}|_{i,j} = \; & \frac{2\varepsilon_0-\Delta t\sigma_y|_{i,j}}{2\varepsilon_0+\Delta t\sigma_y|_{i,j}} E_z^n|_{i,j} \\
& \frac{2\varepsilon_0}{2\varepsilon_0+\Delta t\sigma_y|_{i,j}}\left(D_z^{n+1}|_{i,j}-D_z^n|_{i,j}\right)
\end{aligned}$$

The choice of σ in the absorbing layer is critical for the absorption. Theoretically larger σ result in better absorption. In practice using a large σ in the first (i.e. innermost) PML cells results in large reflection. A more useful approach is to use a small σ in the first PML cells and then to gradually increase the value towards the terminating PEC wall. For example, this can be obtained by:

$$\sigma(\rho) = \sigma_{max}(\frac{\rho}{d})^n$$

where ρ is the depth within the layer and d the thickness of the PML.

C.5 Dispersive media

In dispersive media the constitutive relation for the electric field is:

$$D(\omega) = \varepsilon_0\varepsilon(\omega)E(\omega) \tag{81}$$

The complex relative permittivity is assumed to have the form:

$$\varepsilon(\omega) = \varepsilon_\infty + \chi(\omega) \tag{82}$$

where ε_∞ is the permittivity at infinite frequency and $\chi(\omega)$ the susceptibility function. The corresponding constitutive relation in the time-domain becomes:

$$D(t) = \varepsilon_0\varepsilon_\infty E(t) + \varepsilon_0\int_0^t E(t-\tau)\chi(\tau)\,d\tau \tag{83}$$

Examples of commonly used dispersive models are Debye relaxation:

$$\begin{aligned}\chi(\omega) &= \frac{\varepsilon_s - \varepsilon_\infty}{1 + j\omega t_0} \\ \chi(t) &= \frac{\varepsilon_s - \varepsilon_\infty}{t_0} e^{-t/t_0} u(t)\end{aligned}$$

and Lorentzian resonance:

$$\begin{aligned}\chi(\omega) &= \frac{(\varepsilon_s - \varepsilon_\infty)\omega_0^2}{\omega_0^2 + 2j\omega\delta - \omega^2} \\ \chi(t) &= \frac{(\varepsilon_s - \varepsilon_\infty)\omega_0^2}{\sqrt{\omega_0^2 - \delta^2}} e^{-\delta t} sin(\sqrt{\omega_0^2 - \delta^2} t) u(t)\end{aligned}$$

where $u(t)$ is the unit step function:

$$u(t) = \begin{cases} 1, & t \geq 0 \\ 0, & t < 0 \end{cases}$$

Two different methods for treating dispersive media have been implemented and validated.

Discretizing the convolution in (**??**) results in a summation that is non-local in time. In order to compute it the entire time-history of E has to be known. The recursive convolution approach relies on the fact that for typical dispersive models the convolution may be updated recursively. Realizing this the time-stepping expression for the electric field can be written as:

$$E^{n+1} = \alpha_1 E^n + \alpha_2 \nabla \times H^{n+\frac{1}{2}} + \alpha_3 \psi^n$$

where the running sum variable ψ^n is updated after the electric field according to:

$$\psi^n = \beta_1 E^n + \beta_2 E^{n-1} + \beta_{rec} \psi^{n-1}$$

The first publications of the recursive convolution method [**?**] and [**?**] used a piecewise constant approximation of the convolution sum resulting in only first order accuracy. In a later paper by the same authors [**?**] a second order accurate algorithm using a piecewise linear approximation was introduced. This algorithm called PLRC (piecewise linear recursive convolution) is the one implemented in our code.

In the auxiliary differential equation method, ADE the update procedure is carried out in two steps. The first step is to update the D-field according to the finite difference form of (**??**). In the TM case with $J = 0$ we have:

$$D_z|_{i,j}^{n+1} = D_z|_{i,j}^{n} + \Delta t \left[\frac{H_y|_{i+\frac{1}{2},j}^{n+\frac{1}{2}} - H_y|_{i-\frac{1}{2},j}^{n+\frac{1}{2}}}{\Delta x} - \frac{H_x|_{i,j+\frac{1}{2}}^{n+\frac{1}{2}} - H_x|_{i,j-\frac{1}{2}}^{n+\frac{1}{2}}}{\Delta y} \right]$$

Next, the E-field is updated by solving the constitutive relation as a differential equation in the time-domain. For example, consider the case of Debye relaxation. The constitutive relation in the frequency-domain is:

$$D(\omega) = \varepsilon_0 (\varepsilon_\infty + \frac{\varepsilon_s - \varepsilon_\infty}{1 + j\omega t_0}) E(\omega)$$

Transformation into time-domain using that $j\omega$ becomes $\frac{\partial}{\partial t}$ yields the differential equation:

$$D + t_0 \frac{\partial D}{\partial t} = \varepsilon_0 \varepsilon_s E + t_0 \varepsilon_0 \varepsilon_\infty \frac{\partial E}{\partial t} \tag{84}$$

which is solved using second order accurate central differences:

$$\begin{aligned}Ez|_{i,j}^{n+1} &= \frac{\Delta t + 2t_0}{\varepsilon_0 (2t_0 \varepsilon_\infty + \varepsilon_s \Delta t)} D_z|_{i,j}^{n+1} + \frac{\Delta t - 2t_0}{\varepsilon_0 (2t_0 \varepsilon_\infty + \varepsilon_s \Delta t)} D_z|_{i,j}^{n} \\ &+ \frac{2t_0 \varepsilon_\infty - \varepsilon_s \Delta t}{\varepsilon_0 (2t_0 \varepsilon_\infty + \varepsilon_s \Delta t)} E_z|_{i,j}^{n}\end{aligned} \tag{85}$$

The same approach can be used for other common frequency dependencies such as Lorentzian resonance. The order of the differential equation that has to be solved for E depends on the order of the dispersion model. For example in Lorentz media a second order differential equation has to be solved. In order to get second order accuracy in the finite differences an additional time-level of D consequently is needed.